A multiproxy analysis of extreme wave deposits in a tropical coastal lagoon in Jamaica, West Indies

Suzanne. E. Palmer[1*], Michael. J. Burn[2], and Jonathan Holmes[3]

[1]Department of Life Sciences, The University of the West Indies, Mona Campus, Kingston 7, Jamaica, W.I.
[2]Department of Geography and Geology, The University of the West Indies, Mona Campus, Kingston 7, Jamaica, W.I.
[3]Department of Geography, University College London, UK

*Corresponding author.
E-mail address: suzanne.palmer@uwimona.edu.jm
ORCID: 0000-0002-6247-8291

Declarations

Funding

SP received funds for field work and data analyses from the Department of Geography and Development Studies, University of the Chester (UK), the British Society for Geomorphology (BSG) Research Grant, the British Sedimentological Research Group (BSRG) Gill Harwood Memorial Fund, and the Quaternary Research Association (QRA) Research Fund. MB received funds from the UWI New Initiative Programme and UWI Study and Travel Grant for field work and data analyses.

Conflicts of interest

The authors declare that they have no conflict of interest.

Availability of data and material

Data will be made available from the NOAA's National Centres for Environmental Information (NCEI) (http://www.ncdc.noaa.gov/data-access/paleoclimatology-data/datasets).

Code availability

Not applicable

Authors contributions

SP and MB conceived and designed the study, conducted field work, performed analyses and interpretation on the sedimentogical and geochemical data. JH conceived the design and study of the ostracods, analysed and interpreted the ostracod data. SP and MB prepared the draft manuscript. JH drafted and edited the ostracod data, descriptions, and interpretation. SP, MB and JH reviewed and edited the manuscript. All authors read and approved the final manuscript.

Acknowledgements

We express gratitude to Wijittra Lowaleard for picking, identifying and illustrating ostracod specimens. We are grateful to Ashley Codner for the collection of water chemistry data in January 2014. S.E.P. acknowledges financial support for field work and data analyses from the Department of Geography and Development Studies, University of the Chester (UK), the British Society for Geomorphology (BSG) Research Grant, the British Sedimentological Research Group (BSRG) Gill Harwood Memorial Fund, and the Quaternary Research Association (QRA) Research Fund. M.J.B. acknowledges financial support from the UWI New Initiative Programme and UWI Study and Travel Grant. The authors thank Servel Miller for initiating project discussions and assisting with preliminary observations and photography of sediment cores. We thank Byron Wilson and the Jamaican Iguana Research and Conservation Group for permission to work with them in the Hellshire Hills, Portland Bight Protected Area, and for assistance with transport, field work and logistics. Students and colleagues of the University of the West Indies, Mona are thanked for assisting with core recovery. This manuscript was improved greatly by comments from two anonymous reviewers.

Abstract

The Small Island Developing States (SIDS) of the Caribbean Region are vulnerable to natural hazards including earthquakes, tsunamis and tropical cyclones that can cause widespread devastation. Sedimentary archives of these hazards are often well-preserved in coastal lagoons; however, few studies in the Caribbean have adopted a multiproxy approach to their reconstruction. Here, we present a 1200-year multiproxy record of extreme washover events deposited within a coastal mangrove lagoon on the south coast of Jamaica. Manatee Bay lagoon is a permanent fresh-brackish water mangrove lagoon separated from the Caribbean Sea by a low-elevation carbonate beach. Fifteen sediment cores recovered along five shore-normal transects contain ostracod-rich authigenic carbonate lake muds interspersed with beds of organic lake mud and mangrove peat. The cores contain evidence of multiple palaeo-washover deposits that are readily distinguished by their sedimentology, geochemistry and microsfossil assemblages. Hypersaline conditions dominated the early part of the record (~800–900 CE) and we infer a freshening of lagoonal waters and the subsequent expansion of the mangrove community following an extreme wave event that occurred some time before ~1290–1400 CE. We constrain the primary historical-washover deposit to 1810–1924 cal CE (2σ; 71% probability), a period characterised by extreme tectonic and meteorological events, which include the Great Kingston Earthquake of 1907 and a local episode of enhanced hurricane activity. While the balance of circumstantial evidence indicates the deposit was probably emplaced during the tsunami generated by the 1907 earthquake, we are currently unable to differentiate between tectonically- and meteorologically-driven washover events based on their sedimentological characteristics.

Keywords: Late Holocene, ITRAX µ-XRF, ostracods, extreme washover events, mangrove lagoon, Jamaica.

1. Introduction

The Small Island Developing States (SIDS) of the Caribbean Region are vulnerable to a range of natural hazards that cause significant social and economic losses resulting from damage to infrastructure, homes and livelihoods, and the disruption of agricultural and tourist activities (Collymore, 2011). Extreme wave events associated with storm surges and earthquake-induced submarine landslides are among the most hazardous natural disasters that occur within the region (Prentice et al., 2010). In 2017, Hurricane Irma caused widespread devastation across the Caribbean becoming one of the strongest and costliest hurricanes on record in the tropical Atlantic. The island of Barbuda lost 95% of homes and infrastructure and experienced storm surges of at least 2.4 m above sea level. In Jamaica, the passage of hurricane Dean in 2007 generated storm surge maximum heights of up to 4m and up to two-thirds of homes in Kingston suffered significant damage (Franklin 2008). Similar devastation was caused by the 2010 M_W7.0 earthquake in Haiti, which generated an underwater landslide that produced maximum tsunami heights (flow depth above sea level at tsunami arrival time) of 3m and runup of 1-2m along the south coast of Haiti (Fritz et al., 2010; Lovett 2010; Calais et al., 2010; Hayes et al., 2010) and became a stark reminder of the severe impacts that geological hazards impose on the coastal communities of SIDS in the Caribbean (Hornbach et al., 2010).

While the stochastic nature of tectonically-driven tsunamis generally precludes their prediction, the return-periods for tropical cyclone induced storm-surges are inherently more predictable due to the cyclicity of climatic phenomena. In an attempt to capture this cyclicity and to calculate the return periods of landfalling hurricanes, sedimentological studies aim to identify and count layers of beach sands washed into coastal lagoons during the passage of tropical cyclones (e.g. Liu and Fearn, 2000; Donnelly 2005, Donnelly et al., 2015; Donnelly and Woodruff, 2007, Elsner et al., 2008; Lane et al, 2011; McCloskey and Liu, 2012; Brandon et al, 2013; Toomey et al. 2013; Denommee et al., 2014; Van Hengstum et al., 2014, and see Oliva et al., 2017, 2018; Otvos 2011) and, where appropriate, attempt to differentiate them from those deposited during tsunami events (e.g. Atwater et al., 2012; Engel & Brückner, 2011; Engel et al. 2010, 2012, 2013; Goff et al., 2004, 2011; Ramírez-Herrera et al., 2012; Reinhardt et al., 2011). However, difficulties distinguishing between sand layers emplaced during storms and tsunamis often confound the attribution of washover events to either. Indeed, the false attribution of a sand layer to the passage of a hurricane when actually emplaced during a tsunami, would result in erroneous estimates of the frequency and return periods of storms.

Jamaica has a long and well-documented history of exposure to extreme tectonic and meteorological events since Colonial settlement of the island in 1494 CE. These archival records are found in Spanish and British Colonial and post-Colonial archives as well as within the numerous coastal lagoons that punctuate the country's coastline. The availability of both documentary and environmental archives of natural hazards in Jamaica facilitates the detection of extreme washover events and their attribution to tectonic or climatic causes. Here, we present sedimentological, palaeontological and geochemical evidence of lagoon sediments and extreme washover events deposited in a mangrove lagoon on the south coast of Jamaica. In order to distinguish between events deposited during the passage of tropical cyclones and those emplaced during historically-documented tsunamis, we assess the spatial distribution of the washover events and compare their composition with that of a composite modern analogue washover fan emplaced in 2004 and 2007 by hurricanes Ivan and Dean, respectively.

2. Background

2.1. Natural hazards in Jamaica

Jamaica is bounded by the Caribbean Plate to the South and Gonâve Microplate (Figure 1) to the North and lies within the Main Development Region (MDR) of Atlantic hurricane activity. It is affected by earthquake-generated tsunamis associated with the eastward migration of the Caribbean Plate relative to the North American Plate (Bryant 2014), and the passage of tropical cyclones through the region. Documentary evidence indicates that the Caribbean Region experienced 85 tectonically-induced tsunamis between 1498 and 2006 CE (Harbitz et al., 2012). Jamaica alone has experienced twelve major earthquakes since 1667 CE (Wiggins-Grandison, 2001) including the devastating M_W 7.5 Port Royal earthquake of June 1692 and the M_W 6.5 Great Kingston earthquake of January 1907. The former reportedly caused the sea around Kingston Harbour to retreat 1.6 km and generated a tsunami wave with an estimated wave height of 1.8m (Tomblin and Robson 1977), while the latter produced wave heights up to 2.5m.

Jamaica is centrally located within the Caribbean and experiences a seasonal sub-tropical maritime climate characterized by distinct wet and dry seasons. Temperatures remain constant with an annual average of ~27°C and range of 2–7°C and rainfall and storms are influenced by the seasonal migration of the Hadley Cell, which controls the relative influence of the Intertropical Convergence Zone (ITCZ). Twenty-five tropical cyclones made landfall in Jamaica from 1874-2019 the most recent being Hurricane Sandy, a category 1 hurricane whose eye passed over the study area in November 2012. The most destructive hurricanes to affect Jamaica include hurricanes Gilbert in 1988 (Cat 3, 1.5m storm surge, Clark, 1988), Ivan in 2004 (Cat 4, 1.3-1.5m storm surge), and Dean (Cat 4, 3m storm surge) (Robinson & Khan, 2008) of which only Gilbert made direct landfall. Although hurricanes Ivan, Dean and Matthew (2016; Cat 4, 3 m storm surge southeast coast of Cuba, Stewart, 2017) did not make direct landfall in Jamaica, we observed that the associated storm surges resulted in the deposition of washover deposits along the southern coastline and following Hurricane Ivan (2004) and Dean (2007) the emplacement of distinct washover fans at the study site.

2.2. Study area

Manatee and Coquar Bays are situated within the Portland Bight Protected Area (PBPA) and are bounded to the north by the Hellshire Hills, a karstified 'honeycomb' limestone landscape set within the White Limestone Group of Jamaica (Miller 2004), and to the south by the Caribbean Sea (Figure 2a). Sea grass beds comprising primarily *Thallassia testudinum* occupy soft carbonate muds and sands within the bays and are protected to their south by a fringing reef, which bears the recent scars of the passage of tropical cyclones through the region as well as those of destructive fishing techniques (Aiken et al. 2002). Two permanent coastal mangrove lagoons overlie a coastal karst plateau and are separated from the Caribbean Sea by a narrow (~15-100m) beach comprising fine carbonate sands and a strand community of mixed xerophytic scrub and mangrove vegetation (Figure 2e). The westernmost coastal mangrove lagoon occupies an area of ~1.68 km^2, spans both bays and extends ~0.84 km inland. Dense colonies of red mangroves (*Rhizophora mangle*) grow in clusters within the two lagoons whereas a more diverse mangrove forest comprising the red and black (*Avicennia germinans*) mangroves occupies the littoral zones of the lagoon complex with white (*Laguncularia racemosa*) and buttonwood (*Conocarpus erectus*) mangroves extending into well-drained areas beyond (Woodley, 1971). The halophyte and succulent pioneer species *Batis maritima* occurs along the open margins of the lagoon, and shoreline vegetation including *Sesuvium portulacastrum, Salicornia perennis*, the herbaceous vine *Canavalia maritima* and dune grasses including *Cenchrus tribuloides* are also prominent (Woodley, 1971).

A modern wedge-like washover fan comprising marine bioclastic sand forms an elongated lobe at the southeastern end of the Manatee Bay lagoon which represents the shortest distance between the sea and the lagoon (<100m) (Figure 2c, 2d). The fan presently extends ~150m north- northwestwards into the lagoon. Google Earth imagery taken on March 8th 2006 and November 29th 2007 shows this modern washover fan to be a composite unit most likely emplaced during the passages of Hurricanes Ivan in 2004 and Dean in 2007 (Figure 2b and 2c). Given their respective storm surge heights of 1.5m and 3m, respectively, the fan emplaced during Hurricane Ivan (Figure 2b) was thinner and less extensive spatially than that of Hurricane Dean (Figure 2c). Exploratory core samples of the washover fan revealed a thin band of authigenic carbonate muds separates the two washover fan deposits (Online Resource 5) confirming the occurrence of two separate storm surge events within the washover fan deposit Although the storm surge associated with Hurricane Matthew in 2016 produced washover fans at the study site, these were small and did not extend into the study lagoon. There is no evidence of a modern washover fan at the southwestern end of the lagoon in Coquar Bay.

Rainfall in the Hellshire Hills is mostly restricted to the summer wet season (May-November) as the Intertropical Convergence Zone (ITCZ) influences the region. The southward migration of the ITCZ during the boreal winter enhances the effects of the Bermuda High and results in stronger NE tradewinds and generally arid conditions. Jamaica exhibits a clear response to El Niño Southern Oscillation on interannual timescales typically resulting in drier (wetter) than average conditions during an El Niño (La Niña). Freshwater input to the mangrove lagoons occurs through a combination of direct precipitation and groundwater flow from the surrounding limestone catchment. These waters mix with more saline lagoon waters resulting from saline intrusion, direct washover of sea water from the Caribbean Sea and evaporative concentration. Leaching of organic acids through the peat deposits of the surrounding mangrove ecosystem and the related dissolution of tannins and lignins results in the anoxic clear brown lagoonal waters that are typical of tropical mangrove lagoons (Burn and Palmer, 2014). During the driest months, lake levels retreat and desiccation cracks appear around the perimeter of the lagoon.

The chemistry of the mangrove lagoon waters varies seasonally in response to the changes in the balance between precipitation and evaporation and to variability in the production of humic acids by the surrounding mangrove plant community. Annual field visits between 2010 and 2019 to the Manatee Bay mangrove lagoon were conducted to capture the seasonal variability in water chemistry. Average pH values of 8.5 reflect two competing influences: the basic properties of the underlying limestone geology and the local production of weak organic acids from decaying organic matter. Salinity levels varied significantly during the study period ranging from brackish water conditions (22.64‰) recorded in January 2013 a month after the passage of Hurricane Sandy (Cat 1) in November 2012, to marginally hypersaline conditions (36.94‰) in November 2014 during the two-year Caribbean-wide drought of 2014-2015, the latter value approaching the average salinity of the Caribbean Sea (~36‰). We observed a freshening of lagoonal waters in October 2017 (~10.81‰) following the La Niña event of

2016/2017 where above average rainfall and hurricane activity persisted across the Caribbean. In general, mangrove lagoons exhibit low oxygen levels because dissolved organic substances including tannins and lignins act as reducing agents removing oxygen from the water column. However, the western lagoon at Manatee Bay contains waters that are unusually-well oxygenated exhibiting dissolved oxygen levels ranging from 3.97 mgl^{-1} (68% saturation) during the drought period of 2014-2015, to 7.13 mgl^{-1} (99.1% saturation) in January 2013. Such changes likely reflect the changing seasonal production of oxygen by photosynthetically-active plants and algae combined with the occasional mixing of the water column caused by the passage of tropical cyclones.

3. Methods

3.1. Core recovery and chronology

To capture the spatial distribution of washover events at Manatee Bay, we recovered fifteen short (~1m) sediment cores (MB-1 – MB-15) in October-November 2010 through ~0.4m of water along five shore-normal transects from the western lagoon using a Colinvaux-Vohnout drop-hammer modified piston corer (Colinvaux et al., 1999) (Figure 2d, 3). Two of the fifteen cores were taken directly from the modern washover fan (MB-4 and MB-5), which contains the modern analogue deposits that were emplaced during the passage of Hurricanes Ivan and Dean. Sediment cores were transferred to the laboratory and stored at 4°C before being split and described according to standard core-logging procedures (Schnurrenberger et al., 2003). Sub-samples were collected from seven sediment cores (MB-1, MB-2, MB-4, MB-5, MB-6, MB-13, MB-14) at 1 cm intervals, dried for 1 h at 60°C to establish water content, and analysed for loss-on-ignition at 550°C and 950°C for organic matter and carbonate contents, respectively (Dean, 1974). A total of six Accelerator Mass Spectrometry (AMS) ^{14}C rangefinder dates were obtained from cores MB-1, MB-4, MB-7, and MB-12, from well-preserved and identifiable terrestrial plant macrofossils, bulk organic material and an articulated bivalve of the West Indian pointed venus (*Anomalocardia brasiliana*; Gmelin, 1791), a shallow marine/mangrove lagoon species (Table 1). Samples were treated using a base-acid-base treatment at the Beta Analytic Inc AMS facility in Miami and radiocarbon dates were calibrated using the online software package OxCal 4.2 (Ramsey, 2001). We used the Modeled Ocean Average Marine13 curve to calibrate the conventional ^{14}C date obtained from *A. brasiliana*, and that of IntCal13 (Reimer et al., 2013) for terrestrial samples. Data points are weighted according to the calibrated probabilities and all dates are reported in calibrated calendar years CE (2σ error ranges) (Table 1).

3.2. Geochemical analyses

Seven sediment cores were selected to capture the geochemical variability of the different sedimentary units across the lagoon basin. The seven sediment cores (MB-1, MB-4, MB-5, MB-6, MB-7, MB-12, MB-14) were scanned for X-ray fluorescence using the ITRAX™ micro (μ)-XRF core scanner (Croudace et al., 2006) at Aberystwyth University equipped with a Mo X-ray tube, which was set to 45kV and 50mA. XRF scanning was performed at 1-mm resolution using an integration time of 15s per measurement. The raw geochemical data, measured in intensity counts per second (counts s^{-1}), was normalised by dividing by the total scatter (sum of ITRAX-derived Compton and Raleigh scattered intensities) to minimize the effects of water and organic matter in the sediment matrix (Davies et al. 2015; Kylander et al., 2011). Organic Carbon (OC) was estimated using the ratio of Compton (incoherent) and Raleigh (coherent) scattered intensities (Chagué-Goff et al., 2016; Guyard et al., 2007; Burnett et al., 2011; Jouve et al., 2013; Burn and Palmer, 2014), the fidelity of which was confirmed by comparison with the results of the loss-on-ignition analyses described above (Online Resource 1).

3.3. Ostracod analyses

Sediment core MB-7 was selected to characterise the ostracod assemblages of the lagoon because its location behind the beach barrier is better protected from the direct effects of washover events and contains clear examples of the principal units that are represented in the sediment record (Figure 5, Online Resource 2). The presence and abundance of ostracods are often good indicators of past salinities where populations are in situ and have not been transported. We evaluate these in situ ostracod assemblages to assess the salinity of the lagoon within each of the sedimentary units and to detect any rapid changes in salinity associated with the passage of tropical cyclones and/or tsunamis. Further, we assess the population structure of ostracod assemblages, which can provide insights into the extent of sediment reworking associated with a range of energy conditions within the lagoon (Onlines Resource 3 & 4). For example, fossil assemblages characterised by the presence of adults and a range of juvenile moult stages indicate an in situ population and relatively calm sedimentary environment. In contrast, the absence of juveniles within a given assemblage suggests that the assemblage has been subject to reworking (Whatley, 1988) within a turbulent setting such as during the passage of a storm or tsunami. To this end, we evaluate the ostracod assamblages to characterise the composition and levels of disturbance of ostracod populations of the lagoon during the passage of a hurricane.

Four surface samples and eighteen samples from core MB-7, each of 1 cm^3, were weighed and freeze-dried to disaggregate the sediment and remove the water. Samples were then washed gently with distilled water through 63, 125 and 250µm sieves to remove the fine fraction, and to separate adult and juvenile ostracod shells. Samples were subsequently dried overnight at 40°C prior to re-weighing. Up to 300 specimens (both valves and carapaces) were isolated and picked from the coarsest fraction using a fine nylon brush under the incident light of a low-powered (20×) binocular microscope. Fossil ostracods were sorted onto micropalaeontological slides and counted by species and moult stage. Well-preserved representatives of key species were cleaned using methanol, mounted on Scanning Electron Microscope (SEM) stubs, and gold-coated prior to photography using a Joel JSM-6480LV high performance analytical SEM in the Department of Earth Sciences, University College London. Identification of ostracods was based on the taxonomic descriptions of Sandberg (1964), Sars (1866), Keyser (1975) and Klie

(1933). The ostracod assemblages in core MB-7 were zoned using stratigraphically-constrained cluster analysis by incremental sum of squares (CONISS) with the 'rioja' package in R (Juggins, 2017).

4. Results

4.1. The general depositional environment

The depositional environment of Manatee Bay lagoon comprises predominantly micro-fossil-rich authigenic carbonate lake muds that are punctuated by organic mangrove peat deposits exhibiting varying degrees of decomposition. Poorly decomposed woody fragments exhibit different degrees of decomposition within the carbonate lake muds leaving behind a patchwork of colour ranging from dark to pale yellowish brown within the sediment (Figure 4). The sequence is further punctuated by four stratigraphically distinct carbonate beach sand lenses (Washover Units 1-4), which vary in number across the basin and are readily distinguished by lithology, organic matter content (LOI) and geochemistry (ITRAX). Each of the sand lenses (Washover Units 2-4) contains a mixed-assemblage of fossil marine micro-fauna (beach sands) and lagoon-dwelling ostracod shells (Figure 4), with the exception of the modern washover fan (Washover Unit 1), which is devoid of ostracod shells. These sands are dominated by bioclastic fragments of the green alga *Halimeda* sp., marine foraminifera and coral fragments that are similar compositionally to the carbonate beach sands separating the southern margin of the lagoon from the Caribbean Sea. Here, we describe the sedimentary record based on its sediment geochemistry and ostracod assemblages, followed by a sediment description of the different stratigraphic and washover units (WU1-4) of the Manatee Bay lagoon.

4.2. Geochemical interpretation of ITRAX µXRF elemental scans

Sediment core scans of the most abundant elements Ca, Sr, Fe, Cl, and Br helped distinguish between detrital carbonates (washed-over beach sand lenses comprising marine bioclasts; Ca, Sr), authigenic carbonate (Ca/Sr), and marine organic matter (OC, Br, Fe) (Figure 5). Sr covaries with Ca and has been shown to have a strong affiliation with biogenic calcium carbonate phases (Bishop 1988, Murray & Leinen, 1993). The element is often associated with marine calcitic biota (Chagué-Goff, 2010; Rubio et al., 2000) and has been shown to be a proxy for marine inundation due to its higher concentration in seawater (Chagué-Goff, 2010; Goff et al., 2012). At Manatee Bay, high positive values (~60,000 cps) are associated with the carbonate beach sand lenses, which comprise fossil marine organisms including bioclasts of *Halimeda* sp., coral and mollusc fragments, echinoid spines, sponge spicules and reef benthic foraminifera (Figures 4 and 5). To differentiate geochemically the authigenic lagoon carbonates from allochthonous beach sand lenses, we divide Ca counts by those of Sr (Ca/Sr), which removes the portion of the signal associated with beach sands and emphasizes that of authigenic carbonate production. In general, there is an association between higher Ca/Sr values, which also exhibit low levels of internal signal variability, and the 'purer' authigenic marl sediments, which is readily confirmed by comparison with the sediment lithology (Figure 5 – see bars). Indeed, a Ca/Sr ratio of ~ 4:1 is typical for the purest authigenic carbonates that were precipitated out of the water column. Comparisons between the sediment lithology, the Sr and Ca curves, and the Ca/Sr ratio clearly shows detrital and authigenic forms of carbonate may be readily differentiated geochemically (Figure 5).

The organic carbon (OC) content of sediment cores is estimated by dividing the Compton (incoherent) and Raleigh (coherent) scattered intensities on the basis that the amount of incoherent scattering increases for elements with a lower atomic mass such as carbon (Davies et al. 2015). Comparisons between LOI measurements and ITRAX-derived OC (Online Material 1) confirm the latter may be used as a robust proxy for organic matter. Bromine's propensity to form strong covalent bonds with organic matter has also enabled its use as a proxy for organic content (Kalugin et al. 2007), biological productivity (Gilfedder et al. 2011) and marine spray (storminess; Unkel et al. 2010; Turner et al. 2014). At Manatee Bay lagoon, positive Br excursions are strongly associated with mangrove peats (high OC) and we adopt the elements as proxies for marine organic matter (Figure 5). The absence of the terrigenous detrital indicators Si and Ti within the sediment, suggests that Fe counts, which often co-vary with those of Si and Ti, are not related to the influx of terrestrial material. Instead, we find a strong association between positive excursions of Fe and fragments of the sea grass *Thallassia testudinum* as well as mangrove leaves embedded within the sediment record (Figure 5). Iron-enrichment is common in the leaves of *Thallassia testudinum* (Whelan et al., 2011) and *Rhizophora mangle*; consequently, we suggest that positive excursions in Fe record the rapid burial of iron-rich marine plants washed into the lagoon during storm surge and/or tsunami events. The lack of sedimentary indicators of redox processes (red colouring and iron and manganese concretions) that are typical at nearby Grape Tree Pond (Burn and Palmer, 2014), implies further that the temporal variability in Fe is not influenced significantly by the changing concentrations of oxygen within the lagoon.

4.3. The Ostracod fauna of Manatee Bay Coastal Lagoon

Overall, the fossil ostracod faunas of Manatee Bay lagoon are typical of carbonate, shallow-water coastal environments across the Caribbean (Keyser and Schoning, 2000), which are characterised by significant seasonal variability in salinity ranging from fresh-brackish waters during the wet boreal summer, to hypersaline conditions during the winter dry season. Keyser (1977) showed that the salinity gradient has a strong control on the presence and abundance of different ostracods within coastal carbonate lagoons. Of the four principal ostracods described below, *Heterocypris punctata* thrives generally under fresher conditions with an optimum tolerance range of 3-7‰ and would be expected to flourish during the wetter boreal summer. *Parapontoparta subcaerulea* is an euryhaline species with an optimum salinity range of 8-14‰ that falls within the mesohaline category. In contrast, *Cyprideis edentata* and *Perissocytheridea cribrosa* are adapted to a broader range of salinities and are better able to tolerate hypersaline conditions (>36‰) than *H. punctata* or *P. subcaerulea*. Consequently, the presence and abundance of the above ostracods are a good indicator of past salinities within coastal lagoons across the Caribbean, but only if the populations are in situ and have not been transported. The presence of adults and a range of juvenile moult stages within a fossil assemblage tends to confirm that the populations are in situ whereas the absence of juveniles suggest that the assemblage has been subject to reworking (Whatley, 1988). The second most important control on the ostracod fauna is substrate. In coastal lagoons of the Caribbean, *C. edentata* and *H. punctata* prefer a carbonate mud substrate, *P. cribrosa* is generally found on sandy muds, and *P. subcaerulea* is associated with shelly sands, peat and carbonate muds (Keyser, 1977).

4.3.1. Modern Ostracod Assemblage

Eight ostracod taxa were found in the surface authigenic carbonate sediments. The assemblages in each surface sample were strongly dominated by *Cyprideis edentata* (Klie, 1939) (>80%) with two other taxa, namely *Heterocypris punctata* (Keyser, 1975) and *Perissocytheridea cribrosa* (Klie, 1933), making up a smaller but significant component (<17%). *Parapontoparta subcaerulea* (Keyser, 1975), *Loxoconcha* sp. and 3 other unidentified taxa were found in small numbers. Specimens of *C. edentata* included valves and carapaces, with at least some of their carapaces containing soft parts, suggesting that the individuals had been living at or close to the time of collection. The specimens of *Perissocytheridea cribrosa* also included valves and soft parts, whereas the other species were represented only by valves. The population structure of the surface samples contains adults and 2-3 of the larger juvenile instars (A-1 to A-3) of *C. edentata* and *H. punctata* (Online Resource 4). Taken together, the presence of live ostracod specimens with a population structure containing juvenile instars indicates the assemblage is in situ and exhibits little evidence of sediment reworking.

Cyprideis edentata (Klie 1939) (Figure 7, 1-4)

The genus *Cyprideis* (Jones, 1857) is a holoeuryhaline (freshwater-hypersaline) and eurythermal ostracod genus commonly found in shallow, oligo-mesohaline water including marginal marine environments. It prefers the muddy to mixed mud-sand substrate of lagoons and estuaries (Sandberg, 1964) and is able to tolerate the highly fluctuating salinity conditions typical of coastal lagoon environments, which range from freshwater conditions during the summer rainy season to hypersaline conditions during the dry winter months. (e.g., Sandberg, 1964; Jahn et al.,1996; De Deckker et al., 1999; Meisch, 2000; Frenzel and Boomer, 2005; Gross et al.,2008). Sandberg (1964) and Keyser and Schoning (2000) suggested that *Cyprideis edentata* may be distinguished from other species of *Cyprideis* by the elongate, narrow, multiradiate Y-shaped external openings of the normal pore canals, which also characterize the specimens reported here. Although Medley et al. (2007) suggest that the pore canal shapes of *Cyprideis* are probably a function of the changing salinity of the lagoon and not necessarily species-specific, the large size of the specimens from Manatee Bay (Sandberg, 1964), coupled with the pore-canal morphology, confirm their identification as *C. edentata*. The species has been reported occupying the hypersaline lagoons (recorded salinity 72-90‰) of the Netherlands Antilles (Aruba, Bonaire and Curacao) along the southern margin of the Caribbean Sea (Klie, 1939), Bermuda (Maddocks and Illiffe, 1986) and more recently from Lago Enriquillo of the Dominican Republic in the Greater Antilles (Medley et al., 2007).

Heterocypris punctata Keyser, 1975 (Figure 7, 5-8)

Heterocypris punctata is a nektobenthic ostracod, which is generally found in warm (17-32.5 °C), alkaline (pH 6.5-9.2) and oligo-mesohaline shallow waters (<1 m). Across the Caribbean, its optimum range is associated with authigenic carbonate muds produced within the seasonally fluctuating waters of coastal lagoons (Keyser, 1977; Burn et al. 2016); however, it has also been reported living among dense stands of aquatic macrophytes within the littoral zones of freshwater lakes of Central America (Perez et al., 2010). Keyser and Schoning (2000) reported an optimum salinity range for this species of 2–7‰ (Keyser and Schoning, 2000); however, live specimens collected using grab and tow samples from the study site in Jamaica indicate this species' tolerance range extends to ~22 ‰ (Codner, 2014).

Perissocytheridea cribrosa (Klie, 1933) (Figure 7, 10-12)

Perissocytheridea is a brackish-water genus that is a common inhabitant of coastal and mangrove lagoons across the Caribbean (Martens and Behen, 1994; Keyser, 1977; Malaize et al 2011; Engel et al., 2012, 2013; Perez et al. 2013). *P. cribrosa* is a periphytal euryhaline ostracod that lives in warm (~16.5-34 °C) lagoonal environments with a reported salinity tolerance range of 5-48‰ (Keyser, 1977; Engel et al., 2012; Engel et al., 2013) and a preference for a sandy-mud substrate. While the species is well adapted to the full range of fresh to hypersaline conditions, it is often associated with other euryhaline genera including *Cyprideis* sp. and *Thalassocypria* sp. and exhibits a preference for high-conductivity, polyhaline waters (750µS/cm-55.3mS/cm; Perez et al., 2013, Keyser, 1977). Live specimens were recovered from surficial carbonate muds from Manatee Bay lagoon in January 2013. Spot measurements of water salinity were ~23‰ and conductivity ~36mS/cm (Codner, 2014).

Parapontoparta subcaerulea Keyser, 1975 (Figure 7, 9)

This nektobenthic euryhaline species favours lagoonal environments characterised by rapid changes in salinity (Keyser, 1975). It is found in neo-tropical zones such as littoral, lagoonal, estuarine, sea-grass, and mangrove-wetlands of the coastal areas and is often associated with compacted substrates rich in detritus and sand (Keyser, 1975) and occasionally mangrove peat (Keyser, 1977). The salinity range of *P. subcaerulea* is approximately 3 to 31.0 ‰ (Keyser, 1975) with the maximum abundance occurring between 8.0 and 13.8 ‰ and in water with pH ranging between 6.5 and 9.2 (Keyser, 1977). Live specimens were collected near clusters of red mangroves from Manatee Bay in January 2013 in mesohaline waters with a salinity of 23‰ and conductivity of 36 mS/cm (Codner, 2014).

4.3.2. Ostracod Assemblage Zones

The composition of the fossil ostracod assemblages of core MB-7 varies throughout the core but is commonly dominated by *C. edentata* (≤91%), *H. punctata* (≤65%) and *P. cribrosa* (≤95%)

and smaller proportions of *Parapontoparta subcaerulea*. (Figure 6). The first two of these species are typically represented by adult specimens and a range of juvenile moults, whereas for *P. cribrosa* and *P. subcaerulea*, populations are dominated by adults and A-1 valves (Online Resources 3 & 4).

Five ostracod assemblage zones (OAZs) are identified in core MB-7, numbered OAZ-1 through OAZ-5 (Figure 5). It should be noted that the extent and boundaries of the zones may not be precise in all cases, owing to the variable stratigraphical resolution of the ostracod analyses. OAZ-1 (85-61 cm) is associated with the lower authigenic carbonate muds, has a high ostracod abundance and is dominated by adults and juveniles of *C. edentata* (Online Resource 3), with sporadic occurrences of *H. punctata* (adults and juveniles) and *P. subcaerulea* (adults only). The population structure of this unit is remarkably similar to that of the surface sediment samples (Online Resource 4) suggesting an in situ assemblage. OAZ-2 (60-55 cm) coincides with the sudden transition from authigenic carbonates to the lower organic lake muds and is marked by a significant reduction in the total ostracod abundance driven by a decrease in *C. edentata*. The unit is also characterised by a small rise in *H. punctata* compared with the preceding zone, and the introduction of *P. cribosa*. The population structure indicates these assemblages were found in situ (Online Resource 5). OAZ-3 (52-29 cm) spans the upper organic lake muds and overlying bioclastic sands and is characterised by a general rise in ostracod abundance, driven by a significant increase in *H. punctata* numbers to a maximum at 45cm, followed by a significant decrease, as well as a concomitant increase in the abundance of *C. edentata* and *P. subcaerulia*, which correspond with the bioclastic sand unit between 40-25cm. The only incidence of the marine ostracod genus *Loxoconcha* sp. also occurs within the sand unit at 30cm. OAZ-4 (25-7 cm), which coincides with the upper unit of organic lake muds, is marked by a reduction in ostracod numbers, with assemblages dominated by *C. edentata* and *H. punctata* (adults and juveniles) as well as adults only of *P. cribrosa*. OAZ-5 (5-0 cm) coincides with the recent authigenic carbonates (Online Resource 3). Like the lower authigenic carbonate unit, it contains large numbers of *C. edentata* in the upper level and the lower level in this unit contains significant numbers of adults of *P. cribrosa*.

4.4. The sedimentary units of Manatee Bay lagoon

4.4.1. Authigenic carbonate muds

The lowermost carbonate mud unit spans the entire lagoon and comprises authigenic carbonate lake muds the Munsell colour of which ranges from pinkish gray (5YR 7/3) within the western half of the basin to light yellowish brown (10YR 5/4) in the eastern half. This unit typically exhibits a sharp and distinct upper boundary and a low organic matter content (ca. 10%; Figure 4) although it is punctuated with fine, fibrous root fragments up to several centimeters long. Well-preserved articulated bivalves of the polyhaline species *Anomalocardia brasiliana* occur alongside a range of cerithid gastropods. In core MB-7, the ostracod assemblage (OAZ-1) is dominated by the polyhaline species *C. edentata* (>87%), with lower percentage abundance of the ostracods *H. punctata* (<8%) and *P. subcaerulea* (<8%;) (Fig 5). Note that the first two species are present as adults and juveniles, whereas mainly only adults of the third species were found (Online Material 3 & 4). The sediment geochemistry is characterized by low OC, Br and Fe counts which contrasts with an increase in the Ca/Sr to ~ 4:1 as well as elevated counts of Ca, Sr and Cl. Measurements of radiocarbon activity from well-preserved plant seeds (achenes) recovered from core MB-1, provide a calibrated age range for the base of this unit of 857-989 CE (89-90cm; 89% probability). Similarly, radiocarbon activity from a well-preserved bivalve shell from core MB-7 confirms the approximate age range for this unit with an overlapping calibrated age range of 771-900 CE (90cm; 86% probability; Table 1).

4.4.2. Organic lake muds

The sharp upper boundary of the authigenic carbonate unit provides the transition to the overlying organic lake muds, whose organic matter content ranges from >50% (Schnurrenberger et al., 2003) to lake muds with a reduced organic matter content of ~15-25% and average carbonate content of ~30-35%. ITRAX µXRF scans indicate elevated counts of Br, OC and Ca/Sr, and decreased levels of Ca, Sr and Cl (Figure 5). These lake muds are the most dominant unit within the lagoon sediment record occurring in all cores and often occurs as a gradational unit with subtle up-core changes in colour, carbonate and organic content (Figure 5). The lagoon unit typically comprises brown (10YR/4/3) to dark grayish brown (10YR/4/2), authigenic muds grading up-core to yellowish brown authigenic muds. Fossil microfauna include an array of benthic foraminifera, charophyte oospores and incrustations and brackish water ostracods. The fossil ostracod assemblage is highly variable within this unit (Figure 6), although is typically characterized by a higher abundance of *H. punctata* (ca. 9-65%) than the underlying carbonate unit and lower percentages of *C. edentata* (10-84%) and *P. subcaerulea* (≤6%). The polyhaline ostracod *P. cribrosa* comprises up to ~79% of the ostracod assemblage in contrast to its rarity in the underlying carbonate unit. In contrast, the bivalve *A. brasiliana* and cerithid gastropods are notably absent in the organic lake muds.

4.4.3. Mangrove peat

Mangrove peat accumulation occurs sporadically above the basal carbonate muds; however, it is not spatially continuous and exhibits significant variability in thickness and depth. It generally occurs toward the landward edge and some central areas of the mangrove lagoon, where dense mangrove communities thrive today (MB-1, MB-2, MB-8, MB-9, MB10, MB-11, MB-12, MB-13 (Figure 3). It comprises a coarse, very dark to reddish brown woody mangrove peat with distinct boundaries to over and underlying beds. The organic content (LOI_{550}) is high (average 55% but often exceeding 80%) and can be distinguished by the dominance of large (< 5cm) root, bark and leaf fragments of *Rhizophora mangle* that appear to diffuse red coloration into the surrounding sediment. Geochemically, the unit is characterized by low counts of Ca and Sr and high organic matter content (OC) and Br. Similarly, the carbonate content (LOI_{950}) is lower than that of the underlying carbonate lake muds at ~21%.

4.4.4. Contemporary authigenic carbonate muds

The uppermost sediments of cores recovered beyond the modern washover fan are dominantly composed of authigenic carbonate muds (Figure 3). The thin (~ 5cm) mud unit varies in colour from light yellowish-brown (Munsell) to brown (Munsell) exhibiting average organic (LOI_{550}) and carbonate (LOI_{950}) contents of 36% and 34%, respectively. The unit appears disturbed, containing fragments of rafted leaves that probably originated from the surrounding mangrove communities as well as evidence of mixing with bioclastic marine sands. The percentage of sand within this unit varies spatially across the basin depending on the proximity to the beach barrier and modern washover fan (Washover Unit 1) with higher levels of sand mixed in the authigenic carbonate muds of cores MB1 and MB7 located closer to the barrier. In January 2013 during the boreal winter dry season, Codner (2014) collected surface-sediment and modern water samples from the contemporary authigenic muds and found evidence of live and fossil ostracods dominated by *C. edentata* (64%), *H. punctata* (30%) *P. subcaerulea* (2%) and *P. cribrosa* (4%). This assemblage was associated with average lagoon water salinity measurements of 23‰ and temperatures of 27.1°C. Biostratigraphic analyses of the fossil ostracod fauna found in the surface sediment sample (OAZ-5) from core MB-7 shows similar percentage abundance values of *C. edentata* and *P. cribrosa*; however, neither *H. punctata* nor *P. subcaerulea* were recorded at this level (Figure 5).

4.4.5. Marine washover units

Evidence of multiple palaeo-washover deposits is contained within 13 of the 15 sediment cores recovered from the lagoon (Figure 3). These occur at variable depths and may be identified stratigraphically using a combination of contact boundaries separating the over- and under-lying sediment beds, changes in lithology, sediment geochemistry, bioclastic composition and rapid changes in the fossil ostracod assemblages.

Washover Unit 1 – modern washover unit

The surface of cores MB-4 and MB-5 (0-10cm depth) represent the modern washover fan and comprise white to light-grey white, beach and nearshore carbonate bioclastic sands comprising fine sands with no clasts or debris. These marine bioclastic sands drape over the underlying lagoon muds with a sharp and non-erosional contact (Figure 4), contain low levels of organic matter (<3%) and high carbonate content (>40%). They are readily distinguished by abrupt positive excursions in Ca, Sr and Fe and concomitant declines in organic matter and Br, (Figure 5). This unit is dominated by bioclasts of *Halimeda* sp., echinoid spines, sponge spicules, reef benthic foraminifera and molluscan fragments with the ostracod fauna notably absent (Figure 4). Beyond the modern washover fan Cores MB-1 and MB-6 contain a bioclastic sand unit at ~8-10 cm depth (Figure 3) which we link to the modern washover fan unit (see discussion below).

Washover Unit 2 – ~30-40cm depth

The most distinctive washover unit is well represented in sediment cores MB-1, MB-4 and MB-7 between 30-40 cm depth (Figures 4 & 5). The unit is similar compositionally to its modern analogue counterpart (Washover Unit 1) and is characterized by lenses of fine carbonate sands with an average carbonate content of ~37%; however, with a slightly higher organic content of ~15%. It occurs as a 5-7cm thick, poorly sorted sandy lens of allochthonous marine bioclasts mixed with plant fragments, lagoonal ostracods and charophytes. The unit exhibits increased counts in Sr and Ca, a clear drop in Ca/Sr and significant decreases in the organic matter content as indicated by sudden decreases in the counts of Br and OC (Figure 5). It is characterized by rafted plant fragments including mangrove leaves and rolled-up blades of the sea grass *Thallassia testudinum* that occur within the upper and lower layers of the deposit and correspond with distinctive spikes in Fe counts (Figure 5). In core MB-7, Washover Unit 2 exhibits a clear decrease in adults and juveniles of the fresh-braskish water species *H. punctata*, a corresponding increase in the polyhaline species *C. edentata* (adults and juveniles, Figure 6; Online Resource 3), and the the marine genus *Loxoconcha* sp. is introduced in the upper section of OAZ-3. Further, the fresh-brackish-water charophytes that are typical constituents of the authigenic marl sediments, are notably absent within this unit.

Washover Units 3 & 4

Washover Unit 3 occurs at the transition between the lowermost authigenic carbonate muds and the overlying organic lake muds at a depth of 40cm in MB-4 (Figure 4). The unit is similar compositionally to its modern analogue counterpart (Washover Unit 1) and it comprises light grey to brownish yellow silty sands, marine bioclasts and brackish water charophytes and ostracods (Figure 4). Its occurrence across the basin varies spatially and while there is some evidence of this unit in cores MB-1 and MB-7 at depths of 70cm and 60cm (Figure 3), respectively, there is no clear signature of a washover event observed in the XRF data (Figure 5). However, the ostracod data in core MB-7 (Figure 6) indicate a rapid change in population dynamics from an assemblage dominated by *C. edentata* to one dominated by *H. punctata* and the introduction to the record of *P. cribosa*, which we argue may be indicative of a change in lagoon water chemistry associated with the passage of a storm (See discussion below).

Washover Unit 4 also varies spatially and is detected in the XRF data of core MB-4 (Figure 5) by higher counts in Ca and Sr, a low Ca/Sr ratio, and low levels of Organic Matter. It occurs at the base of core MB-4 (Figure 4), MB-6, MB-13 and MB-15 (Figure 3) and its composition is similar to that of Washover Unit 3 comprising marine bioclasts, and brackish water charophytes and ostracods.

5. Discussion

5.1. Lagoon development over the last ~1200 years

The lowermost unit of the Manatee Bay lagoon cores is characterised by authigenic lake muds deposited since ~800-900 CE (Table 1) that exhibit elevated counts of chlorine, a high Ca/Sr ratio (Figure 5), contain high relative percentages of the salt-tolerant ostracod *C. edentata* (OAZ-1; Figure 6) with a documented salinity range of up to 72-90‰, and the bivalve *A. brasiliana* as well as cerithid gastropod shells. The latter two organisms are common in mangrove lagoons across the Caribbean and have adapted to withstand high salinities (15-80‰ for *A. brasiliana*; 15-44‰ for *Cerithid* gastropod shells; Reinhard et al. 2011). Reinhart et al (2011) found a similar combination of *A. brasiliana* and cerithid gastropod shells in sediments from a coastal lagoon in the British Virgin Islands and interpreted the assemblage as having been deposited under hypersaline and hypoxic conditions. Taken together, the evidence suggests these authigenic muds were therefore emplaced under marine to hypersaline conditions (up to ~44‰) where the evaporative concentration of salts dominated the depositional environment within the lagoon. Today, such conditions are observed annually at the end of the boreal winter dry season in March/April, where water levels subside, lake margins retreat somewhat and salinity increases. The absence of mangrove fragments and peat within this unit may be explained by extended periods of high lagoon-water salinity, which commonly reduces the hydraulic conductivity, leaf water potential, stomatal conductance and photosynthetic rates of *Rhizophora mangle* (Asbridge et al. 2018). Growth suppression and decreases in productivity, propagule production and seedling survival would subsequently result in the contraction of the mangrove forest across the lagoon. The thickness of this unit suggests the site was exposed to an extended deficit of effective moisture that corresponded broadly with the well-documented pan-Caribbean drought that took place during the Terminal Classic Period (800-1000CE) of the Mayan Civilization (Hodell et al. 2001; Evans et al., 2018).

Overlying the authigenic carbonate unit is a spatially consistent sharp transition to organic lake muds and mangrove peats of variable depth and thickness, which corresponds with Washover Unit 3 across the basin and is characterized by the absence of *A. brasiliana*, a significant increase in the relative abundance of *H. punctata* (Figure 6; OAZ-2 and OAZ-3) and concomitant decreases in the abundances of *C. edentata* and *P. subcaerulea*. Although these units are poorly constrained by the available radiocarbon dates, dates recovered from *Ruppia* seeds at 45cm from core MB-7 and at 71cm depth from core MB-12 suggests the unit was deposited around ~1290-1400 CE (Table 1) placing it broadly within the boundaries of the Medieval Climate Anomaly (MCA, ~800-1300CE; Trouet et al., 2009) and the transition period (1300-1450 CE) leading into the Little Ice Age (1450-1850 CE). However, taken together, the ostracod and geochemical (Figure 5) evidence suggests a sudden freshening of lagoonal waters from hypersaline (Figure 6; OAZ-1) to brackish-water (OAZ-2 and 3) conditions occurred at the time of the sharp transition, which cannot readily be explained by longer-term climate variability. Instead, changes in lagoonal dynamics are more likely to have been caused by the passage of a storm or, less-likely, an undocumented tsunami, which re-configured the geomorphology of the lagoon to better capture fresh water and decrease its salinity. Extreme wave events have been demonstrated to influence the geomorphology of coastal lagoons influencing the salinity and subsequent ecological dynamics (Atwater et al., 2012; Engel et al., 2012; 2013). This interpretation is supported further by the presence of Washover Unit 3 in cores MB-2, MB-4, MB5, MB-6, MB-9, MB-10, MB-11, MB-12 (Figure 3) and the influx of marine organic matter transported into the lagoon as a result of mechanical damage to the surrounding sea-grass, mangrove and strand vegetation communities. The latter is characterized in the sediment record by sudden increases in counts of Br and Fe, across the lagoon (E.g. MB-1, MB-7; Figure 5). Concomitant peaks of Fe probably represent the subsequent build-up of decaying plant fragments in the lagoon causing the sediment and decomposing roots to become anoxic, in turn decreasing the redox potential and increasing the concentration of iron-sulfides (pyrite) (Asbridge et al., 2018).

A gradual decline in chlorine counts indicating a progressive freshening of the lagoon from the abrupt transition to the top of the sequence is captured in each of the sediment cores and is best represented in MB-7 (Figure 5). Chlorine counts peak at the abrupt transition (~ 60cm) and decline progressively towards the top of the sequence. While chlorine is often associated with organic matter in micro-XRF studies (Chagué-Goff et al., 2011), variation in the chlorine curve at Manatee Bay occurs independently from changes in the lithostratigraphy suggesting that it does not reflect adsorption onto organic matter but instead is a good geochemical indicator for salinity change. We argue that the salinity spike at the sharp transition between the underlying authigenic carbonate unit and the organic unit above reflects the influx of salt crystals during Washover Unit 3. Subsequent geomorphic changes to the lagoon enabled the progressive capture of fresh water and freshening of the lagoon, an interpretation that is supported by the rapid transition in the dominant ostracod taxa from the hypersaline-tolerant species *C.edentata* in OAZ-1 to the fresh-brackish-water ostracods *H. punctata* and *P. cribosa* in OAZ-2 (Figure 6). The increase in salinity due to sea-water inundation resulting from extreme wave events, negatively impacts mangrove ecosystem development and survival (Asbridge et al., 2018). Further, geomorphic change associated with extreme wave events and the subsequent development of enclosed hypersaline lagoons has been shown to lead to the demise of mangrove populations (Engel et al., 2012, 2013). Therefore, it is possible that the freshening in lagoonal waters at Manatee Bay that occurred above Washover Unit 3, is likely to have promoted the recovery and expansion of the mangrove ecosystem, which is reflected in the development of organic lake muds and mangrove peat layers within the sediment record across the lagoon (E.g. Figure 3; cores MB-1, MB-2, MB-8, MB-9 and MB-10 to MB-14). Such a recovery would have occurred in clusters explaining the variability in the depth and thickness of the organic layers as well as their spatial extent.

5.2. Recent hurricane activity and the modern washover fan

Washover Unit 1

Google Earth imagery taken between March 8th 2006 and Nov 29th 2007 highlights the emplacement of a composite modern washover fan following Hurricanes Ivan (2004) and Dean (2007) revealing that the barrier between the lagoon and the bay was breached by at least two washover events (Figure 2b,c). With the exception of the passage of hurricanes Ivan and Dean to the south of Jamaica in 2004 and 2007 (Franklin 2008; Brennan et al., 2009, Stewart, 2004), no other tropical cyclones can be invoked to explain the deposition of such a distinct lobate sediment fan structure that extended ~150m into the lagoon. Nor indeed, can it be explained by the passage of a tsunami, of which the last such event was documented in 1907. A distinct bipartite sequence of marine sands separated by a thin band of authigenic carbonates at the top of the sediment record (Online Resource 5), supports the attribution of this unit to hurricanes Ivan and Dean. This unit comprises churned-up marine debris originating from the fringing reef and nearshore areas of Manatee Bay and beach sands that were washed into the lagoon across those narrow and vulnerable intervals of the beach barrier least protected by coastal mangrove communities. The thin bed of authigenic carbonate (Online Resource 5) separates the unit supporting the contention that at least two storms were responsible for its deposition.

Direct sedimentological evidence for the modern washover fan is restricted to cores MB-1, MB-4, MB-5 and MB-6 (Figure 3) suggesting not only that the geomorphic impact of the storm surges was limited spatially but also that the lagoon is otherwise well-protected by the fringing reef, beach barrier and extensive mangrove forests. However, the effects of wind-damage to the mangrove forest and the concomitant influx of marine and terrestrial organic matter combined with storm-surge and rainfall related changes in the salinity of the lagoon that are associated with extreme wave events (Asbridge et al., 2018), are also likely to have had a significant impact on the lagoon's ecosystem functioning beyond those locations where geomorphological change is evident. For example, although there is no visible evidence of modern washover sands at the top of cores MB-1, MB-3 and MB-6, the significant positive excursions of Br and Fe clearly record the concurrent influx of marine organic debris, including strands of *Thallassia testudium* and mangrove fragments, into the lagoon (Figure 5). Further, cores MB-1 and MB-6 contain bioclastic sand layers at ~10cm depth, which we interpret as the modern washover fan. Thus, the extreme washover events associated with the passage of hurricanes Ivan and Dean manifest themselves as sandy layers in locations closest to the washover fan (Figure 2d, and authigenic and organic layers comprising marine debris beyond (Figure 3).

5.3. Historical and Palaeo-washover deposits – tropical cyclone or tsunami?

Since ~1200 years BP there have been just four extreme washover events that are recorded within the sediment record the most visible of which are represented in the sediment cores located closest to the beach berm. The presence of marine bioclasts within each of the sand lenses suggests they are allochthonous sediments of marine origin and we interpret these units as extreme wave deposits based on the following common sedimentary characteristics (Mamo et al., 2009; Peters and Jaffe, 2010; Switzer and Jones, 2008; Engel et al., 2016): (i) the presence of $CaCO_3$-rich beach sands containing calcareous marine microfossils and supported by elevated counts of Ca and Sr, (ii) reduced abundance of in situ lagoonal ostracod and charophyte species and (iii) the presence of eroded marine organic fragments incorporated into the lower parts of the deposit and in some instances 'rafted' above the deposit or in the upper layers of the deposit (E.g. MB-7, Figure 5). At Manatee Bay, the rafted allochthonous deposits of marine organic matter are readily detected by their geochemical signature comprising elevated counts of Br and Fe.

Washover Unit 2

The most distinct and spatially extensive event is represented in all cores at ~30-40cm depth constrained broadly by a calibrated radiocarbon date spanning 1691-1730CE (2σ; 24.3% probability) and 1810-1934CE (2σ; 71.1% probability; Table 1) the latter period representing the most likely age range given the > 70% probability that the radiocarbon date falls within this range. Interestingly, these calibrated age ranges span two periods of time within which Colonial and post-Colonial archives document the occurrence of devastating tsunamis. The first was associated with the M_W 7.5 Port Royal earthquake of 1692 and the second with the M_W 6.7 Great Kingston earthquake of 1907 of which the former generated wave run-up heights up to 1.8m that were accompanied by a sea withdrawal of ~1.6 km at Yallahs and the latter wave run-up heights up to 2.5m and a 70-90m withdrawal of the sea at Kingston Harbour (Lander et al., 2002; Taber, 1920).

Given the proximity of the Manatee Bay lagoon to the epicenters of both earthquakes and the generation by each event of significant wave heights of 1.8m and 2.5m, it seems intuitive to surmise that both tsunamis would be represented within the sediment record, particularly when their wave heights are compared with those of Hurricanes Ivan (1.5m) and Dean (3m), which were associated with the emplacement of Washover Unit 1. However, we acknowledege this is not always the case (see Judd et al., 2017 for details). Although the presence of marine bioclasts alone does not enable the differentiation of palaeostorm and palaeotsunami deposits (Morton et al., 2007; Goff et al., 2012; Engel & Brückner, 2011; Switzer & Jones, 2008), Washover Unit 2 comprises marine bioclasts and ostracods (*Loxoconcha* sp.) that are mixed with lagoonal microfossils representing more salt-tolerant ostracod taxa (E.g. *C. edentata*) in OAZ-3 (40-25cm; Figure 6). Arguably, this combination is more likely to occur during the passage and return of a tsunami wave, given its erosive qualities, than during the emplacement of a storm surge washover deposit, which mixes less with the underlying lagoonal sediments (Switzer & Jones, 2008). Our suggested attribution of this event to an earthquake-driven tsunami is further supported by sedimentary evidence of rafted marine organic fragments (e.g. Goff et al., 2011), and associated peaks in iron counts that were incorporated into the lower and upper sections of the deposit and separated by marine sands. We interpret this signal to be a manifestation of the bi-directional flow of a tsunami wave and consequent erosion of the surrounding mangrove and strand vegetation. While some would argue that such a mixed assemblage may also be caused by post-depositional reworking and bioturbation in the lagoon (e.g. as seen by Rhodes et al., 2011; Szczuciński, 2012), the distinct upper contact boundary layers of the unit suggest that disturbance associated with these processes was minimal.

The spatial distribution of washover deposits is often taken into account when attempting to differentiate between storm- and tsunami-induced events. The spatially-restricted lobate and wedge-like sedimentary structure of the Manatee Bay modern washover fan is typical of storm surge deposits that exhibit landward thinning and are rarely continuous across the lagoon. In contrast, washover deposits associated with tsunamis are generally described as sheet-like structures that are spatially consistent across the depositional environment (Engel et al., 2012;

Atwater et al., 2005; Reinhardt et al., 2012; Shanmugam et al., 2012). At Manatee Bay lagoon there are no continuous sandy layers and each of the historical and palaeowashover deposits is restricted to the same areas of the lagoon's southeast quadrant that is most susceptible to the geomorphic effects of tropical cyclones. This would indicate a storm provenance for all such deposits. Moreover, the NOAA hurricane track archives and palaeohurricane reconstructions (Burn et al. 2015; Vecchi & Knutson, 2008, 2011) reveal that the period 1810-1924 CE was particularly active in which three major hurricanes passed within 35nm of Manatee Bay in 1886, 1916 and 1917. Consequently, Washover Unit 2 may alternatively represent a more intense period of hurricane activity during the early 20th Century. Nevertheless, taken together, the sedimentary characteristics of this unit (mixed sediment assemblage, erosional underlying contact, and rafted organic material) as shown in sediment cores MB-1, MB-4 and MB-7 (Figure 5), fulfil the basic criteria for a tsunami deposit following guidelines set out by Switzer and Jones (2008). Further, the unit is chronologically constrained to two windows of time (1691-1730CE; 1810-1934CE) that coincide respectively with tsunami events associated with the historically well-documented Port Royal earthquake of 1692CE and the Great Kingston earthquake of 1907CE. Given the greater probability that the event occurred between 1810-1934CE and the equivocal nature of the sedimentological evidence, we propose that this unit may either represent the first sedimentological evidence of the impacts of the 1907CE earthquake-driven tsunami or the period of intense hurricane activity that occurred in the early 20th Century.

Washover Units 3 & 4

Washover Unit 3 occurs at the transition between the lowermost authigenic carbonate muds between 1290-1400CE and is discussed in detail in Section 5.1 above. Washover Unit 4 is found at the base of the sequence of cores MB-4 (Figure 4), MB-6, MB-13 and MB-15 (Figure 3) located towards the eastern margins of the lagoon. We provide an estimated age older than 768-900 CE (87.5% probability; Table 1) based on the basal radiocarbon date recovered from the lowermost authigenic unit in core MB-7. The unit is similar compositionally to its modern analogue counterpart (Washover Unit 1) and its geochemical composition is similar to that of Washover Unit 3 and is readily differentiated from the overlying authigenic carbonate unit by elevated counts of Ca and Sr and a lower Ca/Sr ratio. Given the higher likelihood of the incidents of storms versus tsunamis and the lack of documentary evidence of a tsunami generated at that time, the unit was probably emplaced during the passage of a tropical cyclone; however, we do not preclude the possibility that this was a tsunami deposit.

6. Conclusion

Given the hazardous consequences of hurricanes and earthquake-generated tsunamis in the Caribbean, we set out to evaluate the timing, spatial distribution and composition (lithostratigraphy, geochemical scans and microfaunal contents) of washover events emplaced in the sediment record of Manatee Bay lagoon, in southern Jamaica. In an attempt to attribute the causes of historical and palaeo-washover layers to either the passage of tropical cyclones or tectonically-generated tsunamis, we compared their composition to that of a modern composite washover fan deposited between 2004 and 2007 during the storm surges associate with the passages of hurricanes Ivan (2004) and Dean (2007). To the same end, we compared the timing of these events with historical records of storms and tsunamis such as the tsunamis generated by the devastating M_W 7.5 Port Royal earthquake of June 1692 and the M_W 6.5 Great Kingston earthquake of January 1907. We found evidence of four washover events, which are characterised broadly by the influx of beach and nearshore bioclastic carbonate sands and marine organic fragments, recorded within the lagoon during the last ~1200 years. Of these, we argue that Washover Unit 2 not only fulfils the basic criteria for a tsunami deposit but also corresponds to the window of time that encapsulated both the 1692 Port Royal Earthquake and 1907 Great Kingston earthquakes, with the range of calibrated radiocarbon ages favouring the latter event with a 71% probability. However, the sedimentological, geochemical and microfaunal evidence are equivocal and may equally represent a sand lens emplaced during a storm surge associated with the passage of a tropical cyclone. The remaining Washover Units 3 (1290-1400 CE) and 4 (before 768-900 CE) are similar compositionally to their modern analogue counterpart (Washover Unit 1) and, given the lack of historical evidence for the occurrence of tsunamis in Jamaica during those times, were most likely emplaced during the passage of tropical cyclones.

While our approach was unable to attribute a specific cause to the historical and palaeo washover events, our multiproxy approach shows promise for the detection of extreme washover events that are not clearly visible within the sediment record (See section 5.1 above). Indeed, reconstructions of hurricane activity based on Loss-on-Ignition or grain-size analyses alone, have been shown to underestimate the return period of tropical cyclones (e.g. Donnelly and Woodruff, 2007; Woodruff et al., 2008) in turn hampering assessments of the natural return periods of tropical cyclones. Given that marine incursion events are often associated with rapid changes in salinity (Engel et al., 2012, 2013), whether it be a freshening of an already hypersaline lagoon or an increase in salinity in a fresh-brackish water lagoon, the improved detection of these rapid changes using a combination of geochemical and microfaunal analyses is likely to improve estimates of the natural return periods of tropical cyclones recovered from tropical lagoon settings across the Caribbean and beyond.

References:

Aiken, K.A., Hay, B., Montemuro, S., 2002. Preliminary assessment of nearshore fishable resources of Jamaica's largest bay, Portland Bight, in: 53rd Gulf and Caribbean Fisheries Institute. pp. 157–176.

Asbridge, S., Lucas, R., Rogers, K., Accad, A. 2018 The extent of mangrove change and potential for recovery following severe Tropical Cyclone Yasi, Hinchinbrook Island, Queensland, Australia. Ecology and Evolution. 8 (21) 10416-10434. https://doi.org/10.1002/ece3.4485

Atwater, B, F., ten Brink, U.S., Buckley, M., et al. 2012. Geomorphic and stratigraphic evidence for an unusual tsunami or storm a few centuries ago at Anegada, British Virgin Islands. Natural Hazards, 63, 51-84. https://doi.org/10.1007/s11069-010-9622-6

Bishop, J. K. B. 1988. The barite-opal-organic-carbon association in oceanic particulate matter. Nature. 332, 341–343.

Brandon CM, Woodruff JD, Lane DP, Donnelly JP. 2013. Tropical cyclone wind speed constraints from resultant storm surge deposition: A 2500-year reconstruction of hurricane activity from St. Marks, FL. Geochemistry, Geophysics, Geosystems 14: 2993–3008. https://doi.org/10.1002/ggge.20217

Brennan, M.J, Knabb R.D, Mainelli, M., Kimberlain, T.B. 2009. Atlantic Hurricane Season of 2007. Monthly Weather Review. 137, 4061-4088.

Bryant, E. 2014. Tsunami: The Underrated Hazard. 3rd Edition. Springer International Publishing. 222 pp.

Burn, M.J. and Palmer, S.E. 2014. Solar forcing of Caribbean drought events during the last millennium. Journal of Quaternary Science. 29 (8), 827-836. https://doi.org/10.1002/jqs.2660

Burn MJ and Palmer SE (2015) Atlantic hurricane activity during the last millennium. Scientific Reports 5: 12838. https://doi.org/10.1038/srep12838

Burn, M., Holmes, L.M., Bain, A., Marshall, J.D., Perdikaris, S. 2016. A sediment-based reconstruction of Caribbean Effective Precipitation during the Little Ice Age from Freshwater Pond, Barbuda. The Holocene. 26 (8) 1237-1247. https://doi.org/10.1177/0959683616638418

Burnett, A., Soreghan, M.J., Scholz, C.A., Brown, E.T. et al., 2011. Tropical East African climate change and its relation to global climate: A record from Lake Tanganyika, Tropical East Africa, over the past 90+ kyr. Palaeogeography, Palaeoclimatology, Palaeoecology. 303 (1–4) 155-167. https://doi.org/10.1016/j.palaeo.2010.02.011

Calais, E., A. Freed, G. Mattioli, F. Amelung, S. Jónsson, P. Jansma, S.-H. Hong, T. Dixon, C. Prépetit, and R. Momplaisir (2010), Transpressional rupture of an unmapped fault during the 2010 Haiti earthquake, Nat. Geosci., 3(11), 794–799. https://doi.org/10.1038/ngeo992

Chagué-Goff, C., 2010. Chemical signatures of palaeotsunamis: A forgotten proxy? Mar. Geol. 271, 67–71. https://doi.org/10.1016/j.margeo.2010.01.010

Chagué-Goff, C., Schneider, J.-L., Goff, J.R., et al., 2011. Expanding the proxy toolkit to help identify past events - Lessons from the 2004 Indian Ocean Tsunami and the 2009 South Pacific Tsunami. Earth-Science Rev. 107, 107–122. http://doi.org/10.1016/j.earscirev.2011.03.007

Chagué-Goff, C., Chan, J., Goff, J. 2016. Late Holocene record of environmental changes, cyclones and tsunamis in a coastal lake, Mangaia, Cook Islands. 25 (5) 333-349. https://doi.org/10.1111/iar.12153

Clark, G. 1988. Preliminary Report Hurricane Gilbert: 08–19 September 1988. 1988 Atlantic Hurricane Season: Atlantic Storm Wallet Digital Archives. National Hurricane Center. p. 10

Codner, A. (2014) Investigation of the modern ostracod assemblage and water chemistry at Manatee Bay Lagoon, Saint Catherine, Jamaica. Undergraduate Thesis, Department of Life Sciences, The University of the West Indies, Mona, Jamaica.

Colinvaux PA, Oliveira PED and Moreno E (1999) Amazon: Pollen Manual and Atlas. London: Harwood Academic Publishers. 344 pp.

Collymore, J. 2011. Disaster management in the Caribbean: Perspectives on institutional capacity reform and development. Environmental Hazards, 10:1, 6-22. https://doi.org/10.3763/ehaz.2011.0002

Croudace, I.W., Rindby, A., Rothwell, R.G. 2006. ITRAX: description and evaluation of a new multi-function X-ray core scanner. Geological Society, London, Special Publications. 267, 51-63. https://doi.org/10.1144/GSL.SP.2006.267.01.04

Davies, S. J., Lamb, H. F., and Roberts, S. J. 2015. Micro-XRF core scanning in palaeolimnology: recent developments. In: Micro-XRF Studies of Sediment Cores, Eds I. W. Croudace and R. G. Rothwell (Dordrecht: Springer), 189–226.

Dean, W., 1974. Determination of carbonate and organic matter in calcareous sediments and sedimentary rocks by loss on ignition; comparison with other methods. J. Sediment. Res. 44, 242–248.

De Deckker, P., Chivas, A.R., Shelley, M.G.J. 1999. Uptake of Mg and Sr in the euryhaline ostracod Cyprideis determined from in vitro experiments. Palaeogeography, Palaeoclimatology, Palaeoecology. 148, 105-116. http://doi.org/10.1016/S0031-0182(98)00178-3

Denommee, K., Bentley, S.J., Droxler, A., 2014. Climatic controls on hurricane patterns: A 1200-year near-annual record from Lighthouse Reef, Belize. Scientific Reports. 4: 3876. Doi: 10.1038/srep03876. https://doi.org/10.1038/srep03876

Donnelly, J.P. 2005, Evidence of past intense tropical cyclones from backbarrier salt pond sediments: A case study from Isla de Culebrita, Puerto Rico, USA. Journal of Coastal Research. 21: 201-210. www.jstor.org/stable/25736985

Donnelly, J.P. and Woodruff J.D., 2007. Intense hurricane activity over the past 5000 years controlled by El Niño and the west African monsoon. Nature. 447 (7143) 465-468. https://doi.org/0.1038/nature05834

Donnelly, J.P., Hawkes, A.D., Lane, P., et al., 2015. Climate forcing of unprecedented intense-hurricane activity in the last 2000 years. Earth's Future. 3 (2) 49-65. https://doi.org/10.1002/2014EF000274

Elsner, J. B., T. H. Jagger, and K.-b. Liu, 2008. Comparison of hurricane return levels using historical and geological records. Journal of Applied Meteorology and Climatology, 47, 368–374. http://doi.org/10.1175/2007JAMC1692.1

Engel, M., Brückner, H., Messenzehl, K., et al. 2012. Shoreline changes in high-energy wave impacts at the leeward coast of Bonaire (Netherlands Antilles). Earth Planets Space. 64, 905-921. https://doi.org/10.5047/eps.2011.08.011

Engel, M., Brückner, H., Fürstenberg, S. et al. 2013 A prehistoric tsunami induced long-lasting ecosystem changes on a semi-arid tropical island - the case of Boka Bartol (Bonaire, Leeward Antilles). Naturwissenschaften. 100, 51–67. https://doi.org/10.1007/s00114-012-0993-2

Engel, M., Brückner, H., Wenrich, V., et al. 2010 Coastal stratigraphies of eastern Bonaire (Netherlands Antilles): New insights into the palaeo-tsunami history of the southern Caribbean. Sedimentary Geology. 231 (1-2) 14-30. https://doi.org/1016/j.sedgeo.2010.08.002

Engel, M., Oetjen, J., May, M. et al. 2016. Tsunami deposits of the Caribbean – Towards an improved coastal hazard assessment. Earth Science Reviews. 163, 260-296. https://doi.org/0.1016/j.earscirev.2016.10.010

Engel, M., Brückner, H. 2011. The identification of paleo-tsunami deposits – a major challenge in coastal sedimentary research. In: Karius, V., Halder, H., Deike, M., vn Eynatten, H., Brückner, H., H., Vött, A. (Eds), Dynamishe Küsten Grundlagen, Zusammenhänge und Auswirkungen im Spiegel angewandter Küstenforschung. Proceedings of the 28th Annual Meeting of the German Working Group on Geography of Oceans and Coasts, 22-25 Apr 2010. Hallig Hooge. Coastline Reports 17, pp. 65-80.

Evans, N.P., Bauska, T.K. et al., 2018. Quantification of drought during the collapse of the classic Maya civilization. Science. 361 (6401) 494-501. https://doi.org/10.1126/science.aas9871

Franklin, J. L., 2008: Tropical Cyclone Report Hurricane Dean. Rep. AL042007, 13–23 August 2007, National Hurricane Center, Miami, FL, 23 pp. Available online at http://www.nhc.noaa.gov/pdf/TCR-AL042007_Dean.pdf.

Frenzel P, Boomer I. 2005. The use of ostracods from marginal marine, brackish waters as bioindicators of modern and quaternary environmental change. Palaeogeography, Palaeoclimatology, Palaeoecology. 225 (1–4) 68–92. https://doi.org/10.1016/j.palaeo.2004.02.051

Fritz. H.M., Hillarie, J.V., Molière, E., et al., 2013. Twin Tsunamis Triggered by the 12 January 2010 Haiti Earthquake. Pure and Applied Geophysics. 170 (9-10) 1463-1474. https://doi.org/10.1007/s00024-012-0479-3

Gilfedder, B.S., Petri, M., Wessel, M., Biester, H. 2011 Bromine species fluxes from Lake Constance's catchment and a preliminary lake mass balance. Geochim et Cosmochim Acta. 75, 3385-3401. https://doi.org/10.1016/j.gca.2011.03.021

Goff, J., Lamarche, G., Pelletier, B. et al. 2011. Predecessors to the 2009 South Pacific tsunami in the Wallis and Futuna archipelago. Earth-Science Reviews. 107, 91. https://doi.org/106. 10.1016/j.earscirev.2010.11.003

Goff, J., Chagué-Goff., Nichol, S., et al. 2012. Progress in palaeotsunami research. Sedimentary Geology. 234-244, 70-88. https://doi.org/1016/j.sedgeo.2011.11.002

Goff, J., McFadgen, B.G., Chagué-Goff, C., 2004. Sedimentary differences between the 2002 Easter storm and the 15th-century Okoropunga tsunami, southeastern North Island, New Zealand. Mar. Geol. 204, 235–250. https://doi.org/10.1016/S0025-3227(03)00352-9

Gross, M., Minati, K., Danielopol, D.L., Piller, W.E. 2008. Environmental changes and diversification of Cyprideis in the Late Miocene of the Styrian Basin (Lake Pannon, Austria). Senckenb Lethaea 88: 161–181. https://doi.org/10.1007/BF03043987

Guyard, H., Chapron, E., St.-Onge, G. et al., 2007. High altitude varve records of abrupt environmental changes and mining activity over the last 4000 years in the Western French Alps (Lake Bramant, Grandes Rousses Massif). Quaternary Science Reviews. 26, 2644-2660. https://doi.org/10.1016/j.quascirev.2007.07.007

Harbitz, C.B., Glimsdal, S., Bazin, S., et al. 2012. Tsunami hazard in the Caribbean: Regional exposure derived from credible worst-case scenarios. Cont. Shelf Res. 38, 1–23. https://doi.org/10.1016/j.csr.2012.02.006

Hayes, G.P., Briggs, R.W., Sladen, A. 2010. Complex rupture during the 12 January 2010 Haiti earthquake. Nature Geoscience. 3 (11) 800–805. https://doi.org/10.1038/ngeo977

Hodell, D.A., Brenner, M., Curtis, J.H., Guilderson, T. 2001 Solar forcing of drought frequency in the Maya lowlands. Science. 292, 1367-1369. https://doi.org/10.1126/science.1057759

Hornbach, M., Braudy, N., Briggs, R. et al. 2010. High tsunami frequency as a result of combined strike-slip faulting and coastal landslides. Nature Geoscience. 3, 783–788. https://doi.org/10.1038/ngeo975

Hornbach, M., Mann, P., Frohlich, C. et al. 2011. Assessing geohazards near Kingston, Jamaica: Initial results from chirp profiling. The Leading Edge. 30, 410-413. https://doi.org/10.1190/1.3575287

Jahn, A., Gamenick, I., Theede, H. 1996. Physiological adaptations of Cyprideis torosa (Crustacea, Ostracoda) to hydrogen sulphide. Marine Ecology Progress Series. 142, 215-223. https://doi.org/10.3354/meps142215

Jones, T. R. 1857. A monograph of the tertiary Entomostraca of England. Monograph of the Palaeontographical Society London. 9: 1-68.

Jouve G, Francus P, Lamoureux S et al. 2013. Microsedimentological characterization using image analysis and µ-XRF as indicators of sedimentary processes and climate changes during Lateglacial at Laguna Potrok Aike, Santa Cruz, Argentina. Quaternary Science Reviews, 71: 191–204. https://doi.org/10.1016/j.quascirev.2012.06.003

Judd, K., Chagué-Goff, C., Goff, J. et al., 2017. Multi-proxy evidence for small historical tsunamis leaving little or no sedimentary record. Marine Geology. 285, 204-215. https://doi.org/10.1016/j.margeo.2017.01.002

Juggins, S. 2017. rioja: Analysis of Quaternary Science Data, R package version (0.9-21). (http://cran.r-project.org/package=rioja)

Kalugin, I., Daryin, A., Smolyaninova, L. et al. 2007. 8000-yr long records of annual air temperature and precipitation over southern Siberia inferred from Teletskoye Lake sediments. Quaternary Research. 67, 400-410. https://doi.org/10.1016/j.yqres.2007.01.007

Keyser (1975) Ostracoden aus den Mangrovegebieten Südwest-Florida (Crustacea: Ostracoda, Podocopa). Abhandlungen und Verhandlungen des Naturwissenschaftlichen Vereins zu Hamburg. 18/19, 255-290.

Keyser, D., 1977. Ecology and zoogeography of recent brackish-water Ostracoda (Crustacea) from South-west Florida. In Löffler, H. & D. Danielopol (eds.) Aspects of the Ecology and Zoogeography of Recent and Fossil Ostracoda. Dr. W. Junk Publishers, The Hague: 207–222.

Keyser, D. and Schoning, C. (2000) Holocene ostracoda (crustacea) from Bermuda. Senckenbergiana lethaea. 80, 567-591.

Klie, W. 1933. Zoologische Ergebnisse einer Reise nach Bonaire, Curacao und Aruba im Jahre 1930 NB 5.Süßwasser-und Brackwasser-Ostracoden von Bonaire, Curacao und Aruba. Zoologisches J, 64 (5), 369-390

Klie, W. 1939. Ostracoden aus den marinen Salinen von Bonaire, Curacao und Aruba. Capita Zoologica. 8 (42) 1-19.

Kylander, M.E., Lind, E.M., Wastegård, S., Löwemark, L. 2011 Recommendations for using XRF core scanning as a tool in tephrochronoloy. The Holocene. 22 (3) 371-375. https://doi.org/10.1177/0959683611423688

Lander, J., Whiteside, L., Lockridge, P. 2002. A brief history of tsunamis in the Caribbean Sea. Science of Tsunami Hazards. 20 (1) 57-94.

Lane, P., Donnelly, J.P., Woodruff, J.D. et al., 2011. A decadally-resolved paleohurricane record archived in the late Holocene sediments of a Florida sinkhole. Marine Geology. 287 (1-4) 14-30. https://doi.org/10.1016/j.margeo.2011.07.001

Liu, K.B. and Fearn, M.L. 2000. Reconstruction of prehistoric land-fall frequencies of catastrophic hurricanes in northwestern Florida from lake sediment records. Quaternary Research. 54 (2) 238-245. https://doi.org/10.1006/qres.2000.2166

Lovett, R. A. 2010. Haiti earthquake produced deadly tsunami. Nature Journal. doi:10.1038/news.2010.93. Available online at: www.nature.com/news/2010/100225/full/news.2010.93.html. Last accessed 15 November 2019.

Maddocks, R. F. and Iliffe, T. M. (1986). Podocopid Ostracoda of Bermudian caves. Stygologia. 2: 26-76

Malaize, B., Bertran, P., Carbonel, P., et al., 2011. Hurricanes and climate in the Caribbean during the past 3700 years BP. The Holocene. 21 (6) 911-924. https://doi.org/10.1177/0959683611400198

Mamo, B., Strotz, L., Dominey-Howes, D., 2009. Tsunami sediments and their foraminiferal assemblages. Earth-Science Rev. 96, 263–278. https://doi.org/10.1016/j.earscirev.2009.06.007

Martens, K. & Behen, F. 1994. A checklist of the recent non-marine ostracods (Crustacea, Ostracoda) from the inland waters of South America and adjacent islands. Travaux scientifiques du Musée d’Histoire Naturelle de Luxembourg, 22: 1-84.

McCloskey and Liu, 2012. A sedimentary-based history of hurricane strikes on the southern Caribbean coast of Nicaragua. Quaternary Research. 78 (3) 454-464. https://doi.org/10.1016/j.yqres.2012.07.003

Medley, P., Tibert, N.E., Patterson, W.P. et al 2007. Paleosalinity history of middle Holocene lagoonal and lacustrine deposits in the Enriquillo Valley, Dominican Republic based on pore morphometrics and isotope geochemistry of Ostracoda. Micropaleontology, 53 (5) 409-419. https://doi.org/10.2113/gsmicropal.53.5.409

Meisch C. 2000. Freshwater Ostracoda of western and central Europe. Berlin: Springer.

Miller, D. J. 2004. Karst Geomorphology of the White Limestone Group. Cainozoic Research, 3, 189- 219.

Morton, R.A., Gelfenbaum, G., Jaffe, B.E. 2007. Physical criteria for distinguishing sandy tsunami and storm deposits using modern examples. Sedimentary Geology 200: 184–207. https://doi.org/10.1016/j.sedgeo.2007.01.003

Muhs, D.R., et al. 2017. Late Quaternary uplift along the North America-Caribbean plate boundary: Evidence from the sea level record of Guantanamo Bay, Cuba. Quaternary Science Reviews. 178, 54-76.

Murray, R. W., and M. Leinen (1993a) Chemical transport to the seafloor of the equatorial Pacific Ocean across a latitudinal transect at 135°W: Tracking sedimentary major, trace, and rare earth element fluxes at the equator and the Intertropical Convergence Zone, Geochim. Cosmochim. Acta. 57, 4141– 4163.

Oliva, F., Perso, M., Viau, A. 2017. A review of the spatial distribution of and analytical techniquies used in paleotempestological studies in the western North Atlantic Basin. Progress in Physical Geography. 1-20. https://doi.org/10.1177/0309133316683899

Oliva, F., Viau, A.E., Peros, M.C., Bouchard, M. 2018. Paleotempestology database for the western North Atlantic basin. The Holocene. 1-8. https://doi.org/10.1177/0309133316683899

Otvos, E.G. 2011. Hurricane signatures and landforms – towards improved interpretations and global storm climate chronology. Sedimentary Geology. 239, 10-22. https://doi.org/10.1016/j.sedgeo.2011.04.014

Perez, L., Lorenschat, J., Brenner, M., et al., 2010. Extant freshwater ostracodes (Crustacea: Ostracoda) from Lago Petén Itzá, Guatemala. Rev. Biol. Trop. 58 (3) 871-895.

Pérez, L., Lorenschat, J., Massaferro, J. et al. 2013. Bioindicators of climate and trophic state in lowland and highland aquatic ecosystems of the Northern Neotropics. Revista de Biología Tropical, Universidad de Costa Rica. 61 (2) 603-644.

Peters, R., Jaffe, B., 2010. Identification of Tsunami Deposits in the Geologic Record; Developing Criteria Using Recent Tsunami Deposits. U.S. Geological Survey Open-File Report 2010-1239, 39p. https://doi.org/10.3133/ofr20101239

Prentice, C., P. Mann, A. J. Crone, R. D. Gold, K. W. Hudnut, R. W. Briggs, R. D. Koehler, and P. Jean (2010), Seismic hazard of the Enriquillo–Plantain Garden fault in Haiti inferred from palaeoseismology, Nat. Geosci., 3, 789–793. https://doi.org/10.1038/ngeo991

Ramírez-Herrera, M.-T., Lagos, M., Hutchinson, I., et al., 2012. Extreme wave deposits on the Pacific coast of Mexico: Tsunamis or storms? A multi-proxy approach. Geomorphology 139-140, 360–371. https://doi.org/10.1016/j.geomorph.2011.11.002

Reimer, P. J., Bard, E., Bayliss, A., et al. 2013. IntCal13 and Marine13 Radiocarbon Age Calibration Curves 0-50,000 Years cal BP. Radiocarbon 55 (4) 1869-1887. https://doi.org/10.2458/azu_js_rc.55.16947

Reinhardt, E.G., Pilarczyk, J., Brown, A., 2011. Probable tsunami origin for a Shell and Sand Sheet from marine ponds on Anegada, British Virgin Islands. Nat. Hazards 63, 101–117. https://doi.org/10.1007/s11069-011-9730-y

Rhodes, B.P., Kirby, M.E., Jankaew, K., Choowong, M. 2011. Evidence for a mid-Holocene tsunami deposit along the Andaman coast of Thailand preserved in a mangrove environment. Marine Geology. 282, 255-267. https://doi.org/10.1016/j.margeo.2011.03.003

Robinson, T. and Khan, S. 2008. Physical Assessment of Post-Hurricane Dean Shoreline Damage and Changes in Jamaica. Report to the Environmental Foundation of Jamaica. pp137

Rubio, B, Nombela, M.A., Vilas, F. 2000. Geochemistry of Major and Trace Elements in Sediments of the Ria de Vigo (NW Spain): an Assessment of Metal Pollution. Marine Pollution Bulletin. 40 (11) 968-980. https://doi.org/10.1016/S0025-326X(00)00039-4

Sandberg, P.A. 1964a. The ostracod genus Cyprideis in the Americas. Stockholm Contributions in Geology. 12, 1–178.

Sars, G.O. 1866. Oversigt af Norges marine Ostracoder. Forhandlinger i Videnskabs-Selskabet i Christiania. 1, 1-130.

Schnurrenberger, D., Russell, J., Kelts, K. 2003. Classification of lacustrine sediments based on sedimentary components. Journal of Paleolimnology. 29, 141-154. https://doi.org/10.1023/A:1023270324800

Shanmugam, G. 2012. Process-sedimentological challenges in distinguishing paleo-tsunami deposits. Nature Hazards. 63, 5-30. https://doi.org/10.1007/s11069-011-9766-z

Stewart, S. 2004: Tropical Cyclone Report Hurricane Ivan. Rep. AL092004, 2-24 Sepetmber 2014, National Hurricane Center, Miami, FL, 44 pp. Available online at https://www.nhc.noaa.gov/data/tcr/AL092004_Ivan.pdf

Stewart, S. 2017: Tropical Cyclone Report Hurricane Matthew. Rep. AL142016, 28 Sepetmber – 9 October 2016, National Hurricane Center, Miami, FL, 96 pp. Available online at https://www.nhc.noaa.gov/data/tcr/AL142016_Matthew.pdf

Switzer, A.D., Jones, B.G., 2008. Setup, Deposition, and Sedimentary Characteristics of Two Storm Overwash Deposits, Abrahams Bosom Beach, Southeastern Australia. J. Coast. Res. 1, 189–200. https://doi.org/10.2112/05-0487.1

Szczuciński, W. 2012. The post-depositional changes of the onshore 2004 tsunami deposits on the Andaman Sea coast of Thailand. Natural Hazards 60, 115–133. https://doi.org/10.1007/s11069-011-9956-8

Taber, S., 1920. Jamaica earthquakes and the Bartlett Trough. Bull. Seismol. Soc. Am. 10, 55–89.

Tomblin, J. M. and Robson, G. R., 1977. A Catalogue of Felt Earthquakes for Jamaica with reference to other islands in the Greater Antilles. Mines and Geology Division, Ministry of Mining and Natural Resources. Special Publication No. 2. 243 pp. Kingston, Jamaica.

Toomey, M. R., Curry, W. B., Donnelly, J. P., van Hengstum, P. J. Reconstructing 7000 years of North Atlantic hurricane variability using deep-sea sediment cores from the western Great Bahama Bank. Paleoceanography 28, 31–41 (2013). https://doi.org/10.1002/palo.20012

Trouet, V. et al. 2009. Persistent Positive North Atlantic Oscillation Mode Dominated the Medieval Climate Anomaly. Science. 324, 78. https://doi.org/10.1126/science.1166349

Turner, T.E., Swindles, G., Roucoux, K. 2014 Late Holocene ecohydrological and carbon dynamic of a UK raised bog: impact of human activity and climate change. Quaternary Science Reviews. 84, 65-85. https://doi.org/10.1016/j.quascirev.2013.10.030

Unkel, I., Fernandex, M., Björk, S., Ljung, K., Wohlfarth, B. 2010. Records of environmental changes during the Holocene from Isla de los Estados (54.4°S), southeastern Tierra del Fuego. Global Planetary Change. 74, 99-113. https://doi.org/10.1016/j.gloplacha.2010.07.003

Van Hengstum PJ, Donnelly JP, Toomey MR et al. (2014) Heightened hurricane activity on the Little Bahama Bank from 1350 to 1650 AD. Continental Shelf Research 86: 103–115. https://doi.org/10.1016/j.csr.2013.04.032

Vecchi, G. A., Knutson, T.R. 2008. On estimates of historical North Atlantic tropical cyclone activity. Journal of Climate. 21, 3580–3600. https://doi.org/10.1175/2008JCLI2178.1

Vecchi G. A., Knutson T. R. 2011. Estimating annual numbers of Atlantic hurricanes missing from the HURDAT database (1878–1965) using ship track density. Journal of Climate. 24, 1736–1746. https://doi.org/10.1175/2010JCLI3810.1

Whatley, R.C., 1988. Population structure of ostracods: some general principles for the recogntion of palaeoenvironments. In: De Deckker, P., Colin, J.P., Peypouquet, J.P. (Eds.), Ostracoda in the Earth Sciences. Elsevier, pp. 245-256.

Whelan, III, T, Van Tussenbroek, B.I., Barba Santos, M.G. 2011. Changes in trace metals in Thalassia testudinum after hurricane impacts. Marine Pollution Bulletin. 62, 2797-2802. https://doi.org/10.1016/j.marpolbul.2011.09.007

Wiggins-Grandison, M.D. 2001. Preliminary Results from the New Jamaica Seismograph Network. Seismological Research Letters. 72 (5) 525-537. https://doi.org/10.1785/gssrl.72.5.525

Woodley, J.D., 1971. Hellshire Hills Scientific Survey, 1970. Kingston, Jamaica.

Woodruff, J. D., et al., 2008. Assessing sedimentary records of paleohurricane activity using modeled hurricane climatology. Geochem. Geophys. Geosyst., 9, Q09V10, https://doi.org/ 10.1029/2008GC002043

Fig. 1 The tectonic plate boundaries of the Caribbean Region and surrounding areas. The plate boundaries are redrawn from Muhs et al. (2017). The location of the study areas, Jamaica is shown (red box). EPGFZ: Enriquillo-Plantain Garden fault zone, WFZ: Walton fault zone , GMP: Gonâve Microplate. Figure created in Adobe Illustrator 2019.

Fig. 2 Location map of Manatee Bay. Maps showing: (a) the location of Manatee Bay in Hellshire Hills on the southeast coast of Jamaica, (b) an aerial Google Earth satellite image dated 03.08.2006 showing the location and extent of the washover fan prior to Hurricane Dean, and likely emplaced by Hurricane Ivan (c) an aerial Google Earth satellite image dated 29.01.2010 showing the location and extent of the washover fan which was emplaced following Hurricane Dean, (d) the location of the piston sediment cores recovered from the Manatee Bay lagoon in October-November 2010, and the location of the modern washover fan in c, d, and e (red box),

(e) an oblique view looking south east over the modern washover fan which is located at the eastern edge of the lagoon. Image taken November 2010. Figure created in Adobe Illustrator 2019

Fig. 3 Diagram illustrating the location of cores recovered across transects. Sedimentary logs for each core are shown highlighting the location of the Washover Units as well as the location of radiocarbon dated samples presented in calendar years BP (cal YBP). Figure created in Adobe Illustrator 2019

Fig. 4 Core image, log and sediment description of sediment core MB-4. The four Washover Units (1-4) are distinguished based on the composition of the sediment specifically carbonate and organic content, Munsell color, skeletal constituents, ostraocods. Figure created in Adobe Illustrator 2019

Fig. 5 Core image, log and sediment description of sediment cores MB-1, MB-4, and MB-7 plotted alongshore the full μ-XRF scans for strontium (Sr), calcium (Ca), the ratio of sedimentary calcium to strontium (Ca/Sr), organic carbon (inc/coh), bromine (Br), iron (Fe), chlorine (Cl). All elemental profiles are presented as normalized units and organic carbon was measured using the ratio of Compton and Raleigh scattered intensities. Figure created in Adobe Illustrator 2019

Fig. 6 Ostracod Assemblage Zones (OAZ) 1-5 for Core MB-7 as determined using stratigraphically-constrained cluster analyses. Ostracod counts represent the number of specimens (valves and carapaces) counted per 1cm^3 at each sampled depth.

Fig. 7 SEM images of ostracod specimens from Manatee Bay. L = length, H = height (both in mm); RV = right valve, LV = left valve. Arrows point in anterior direction. (1-5) *Cyprideis edentata*, (1) male external lateral view of RV, L=1.024, H=0.53. (2) male external lateral view of LV, L=1.091, H=0.573. (3) female external lateral view of LV, L=0.974, H=0.563) X 110, (4) female, dorsal view of carapace, L=1.011, H=0.502. (5-8) *Heterocypris punctata*, (5) internal lateral view of LV, L=1.294, H=0.796. (6) external lateral view of RV of A-1 instar, L=1.128, H=0.68. (7) external lateral view of LV of A-4 instar, L=0.669, H=0.407. (8) Dorsal view of carapace of A-3 instar, L=0.777, H=0.36. (9) *Parapontoparta subcaerulea* Carapace, RV visible, L=0.584, H=0.299. (10-12) *Perissocytheridea cribrosa*, (10) external lateral view of female LV, L=0.507, H=0.29. (11) female, dorsal view of carapace, L=0.52, H=0.282) X 220. (12) male external lateral view of LV, L=0.538, H=0.272

Table 1 Radiocarbon dates for the last 1200 calibrated years from the Manatee Bay sediment record. Dates marked in bold are more strongly weighted in the age depth model

Online Resource 1 Core MB-4 image, log and plots of LOI_{950} (% carbonates), LOI_{550} (% organics) and ITRAX-derived organic carbon counts (Compton (incoherent) and Raleigh (coherent) scattered intensities) and Bromine (Br) counts.

Online Resource 2 Core image, log and sediment description of sediment core MB-7 based on the composition of the sediment specifically carbonate and organic content, Munsell color and skeletal constituents.

Online Resource 3 Ontogeny of the four main ostracod species from each of the sampled depth ranges in core MB-7 illustrating the Ostracod Assemblage Zones (OAZ) 1-5. Counts represent the number of specimens (valves and carapaces) counted for each species and moult stage (A – A-5) within a 1 cm^3 sample.

Online Resource 4 Ontogeny of the four main ostracod species from surface samples from core MB-7. Counts represent the total number of specimens (valves and carapaces) counted for each species and moult stage (A – A-5) within a 1 cm^3 sample.

Online Resource 5 Image of exploratory core samples of the washover fan revealing a thin band of authigenic carbonate muds separateing the two washover fan deposits at the top of the core.

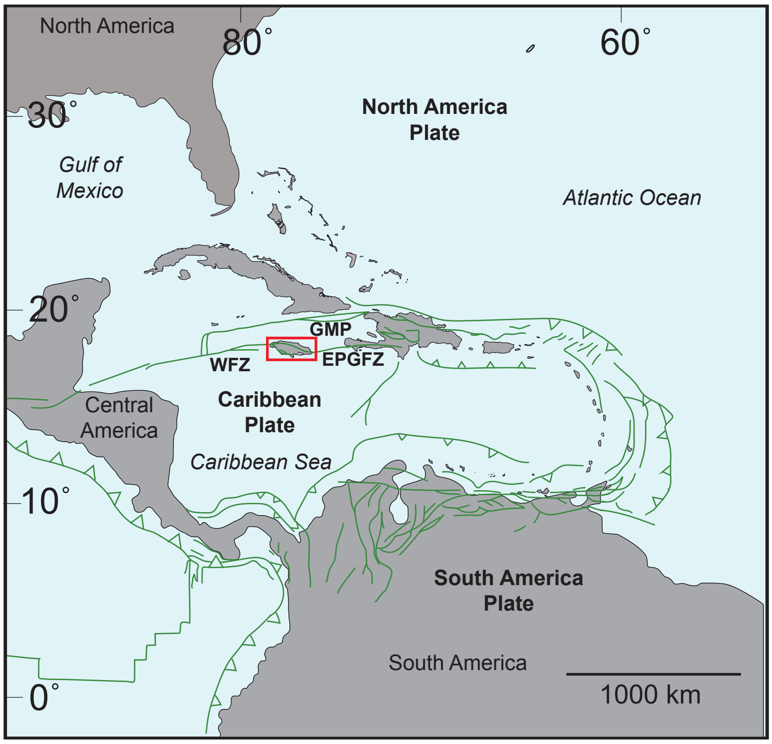
North America
80°
60°
30°
North America
Plate
Gulf of
Mexico
Atlantic Ocean
20°
GMP
WFZ
EPGFZ
Caribbean
Plate
Central
America
Caribbean Sea
10°
South America
Plate
South America
1000 km
0°

Figure 1

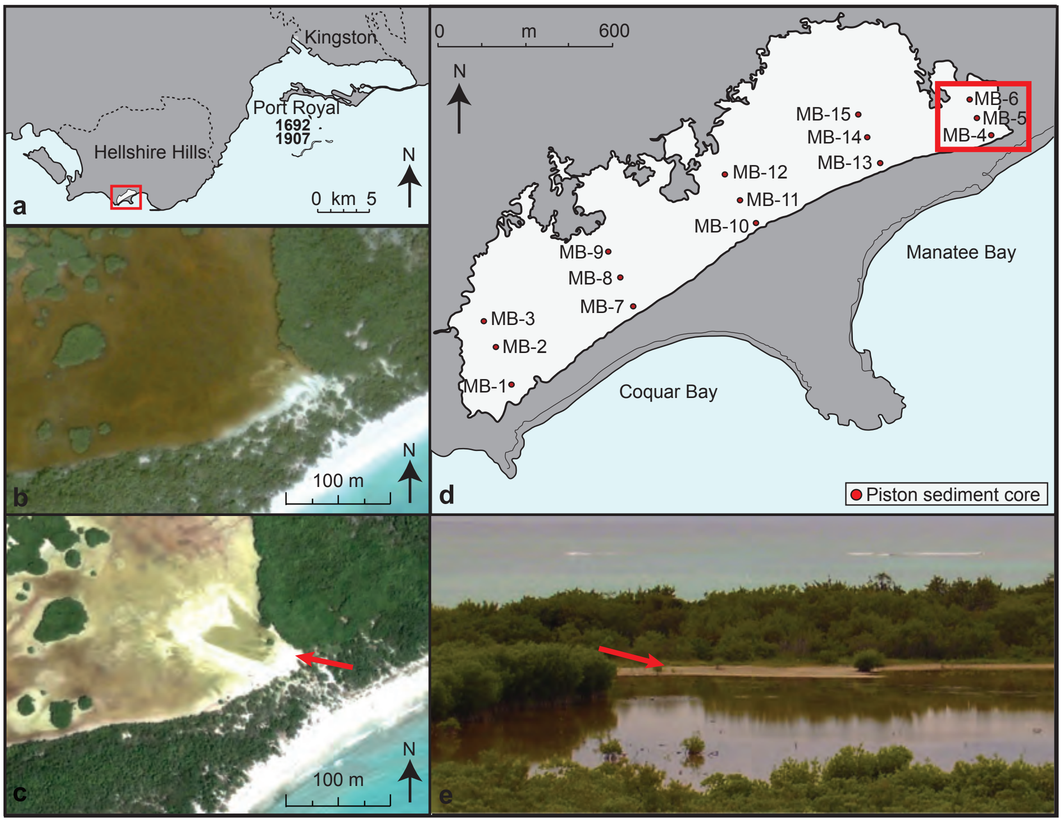

Figure 2

https://nsf.gov/news/mmg/mmg_disp.jsp?med_id=68470&from=

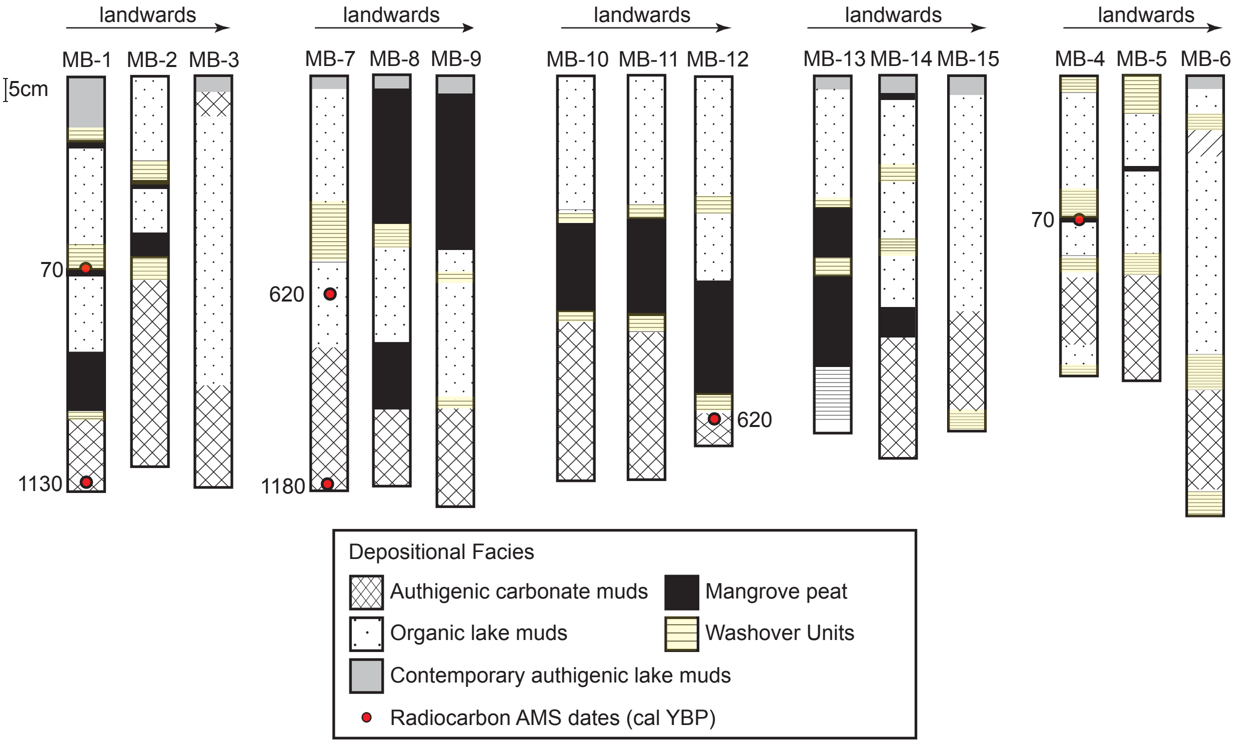
landwards
MB-1
MB-2
MB-3
landwards
MB-7
MB-8
MB-9
landwards
MB-10
MB-11
MB-12
landwards
MB-13
MB-14
MB-15
landwards
MB-4
MB-5
MB-6
5cm
70
1130
620
1180
620
70
Depositional Facies
Authigenic carbonate muds
Mangrove peat
Organic lake muds
Washover Units
Contemporary authigenic lake muds
Radiocarbon AMS dates (cal YBP)

Figure 3

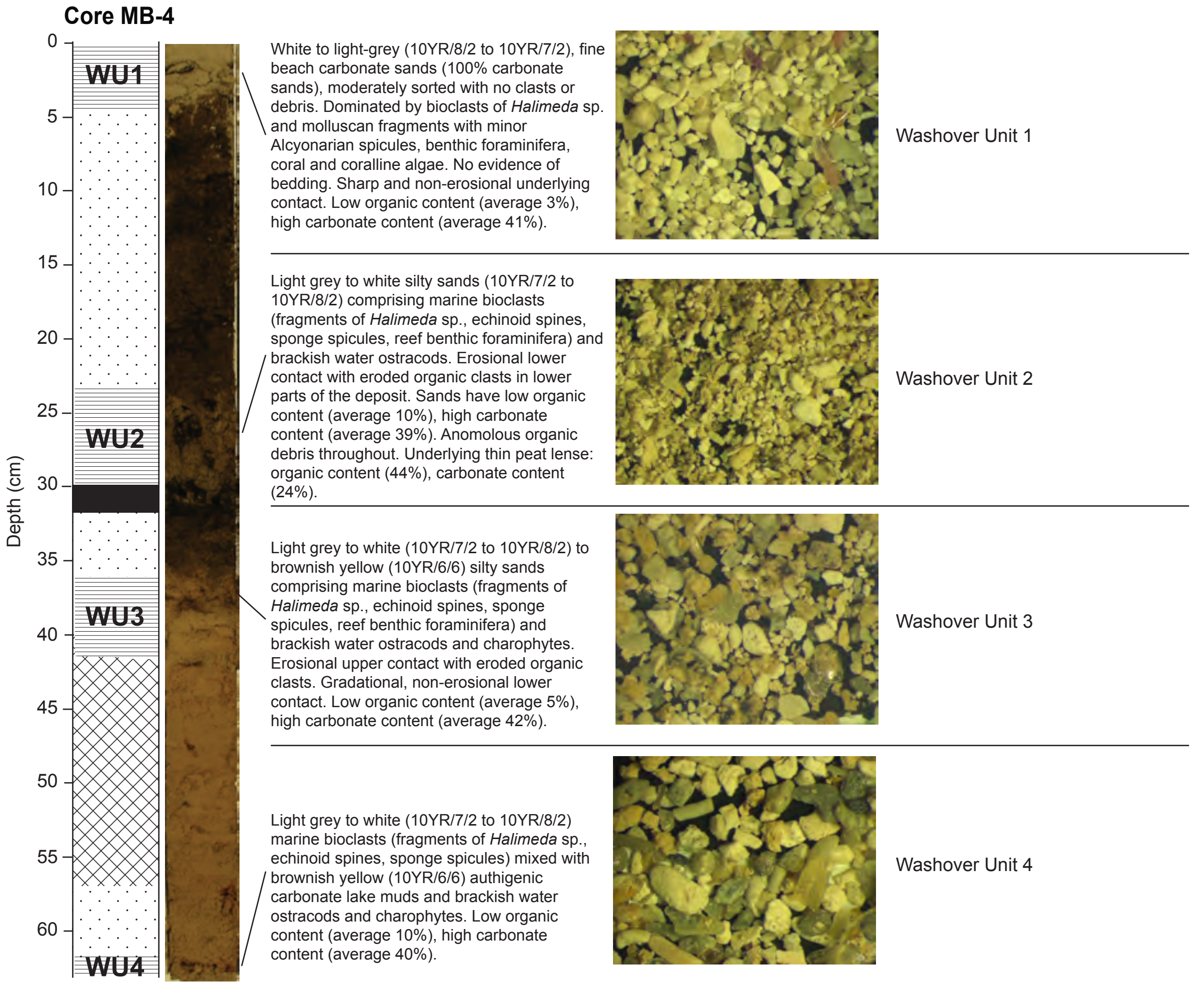
Core MB-4
Depth (cm)
0
5
10
15
20
25
30
35
40
45
50
55
60
WU1
WU2
WU3
WU4
White to light-grey (10YR/8/2 to 10YR/7/2), fine beach carbonate sands (100% carbonate sands), moderately sorted with no clasts or debris. Dominated by bioclasts of *Halimeda* sp. and molluscan fragments with minor Alcyonarian spicules, benthic foraminifera, coral and coralline algae. No evidence of bedding. Sharp and non-erosional underlying contact. Low organic content (average 3%), high carbonate content (average 41%).
Washover Unit 1
Light grey to white silty sands (10YR/7/2 to 10YR/8/2) comprising marine bioclasts (fragments of *Halimeda* sp., echinoid spines, sponge spicules, reef benthic foraminifera) and brackish water ostracods. Erosional lower contact with eroded organic clasts in lower parts of the deposit. Sands have low organic content (average 10%), high carbonate content (average 39%). Anomolous organic debris throughout. Underlying thin peat lense: organic content (44%), carbonate content (24%).
Washover Unit 2
Light grey to white (10YR/7/2 to 10YR/8/2) to brownish yellow (10YR/6/6) silty sands comprising marine bioclasts (fragments of *Halimeda* sp., echinoid spines, sponge spicules, reef benthic foraminifera) and brackish water ostracods and charophytes. Erosional upper contact with eroded organic clasts. Gradational, non-erosional lower contact. Low organic content (average 5%), high carbonate content (average 42%).
Washover Unit 3
Light grey to white (10YR/7/2 to 10YR/8/2) marine bioclasts (fragments of *Halimeda* sp., echinoid spines, sponge spicules) mixed with brownish yellow (10YR/6/6) authigenic carbonate lake muds and brackish water ostracods and charophytes. Low organic content (average 10%), high carbonate content (average 40%).
Washover Unit 4

Figure 4

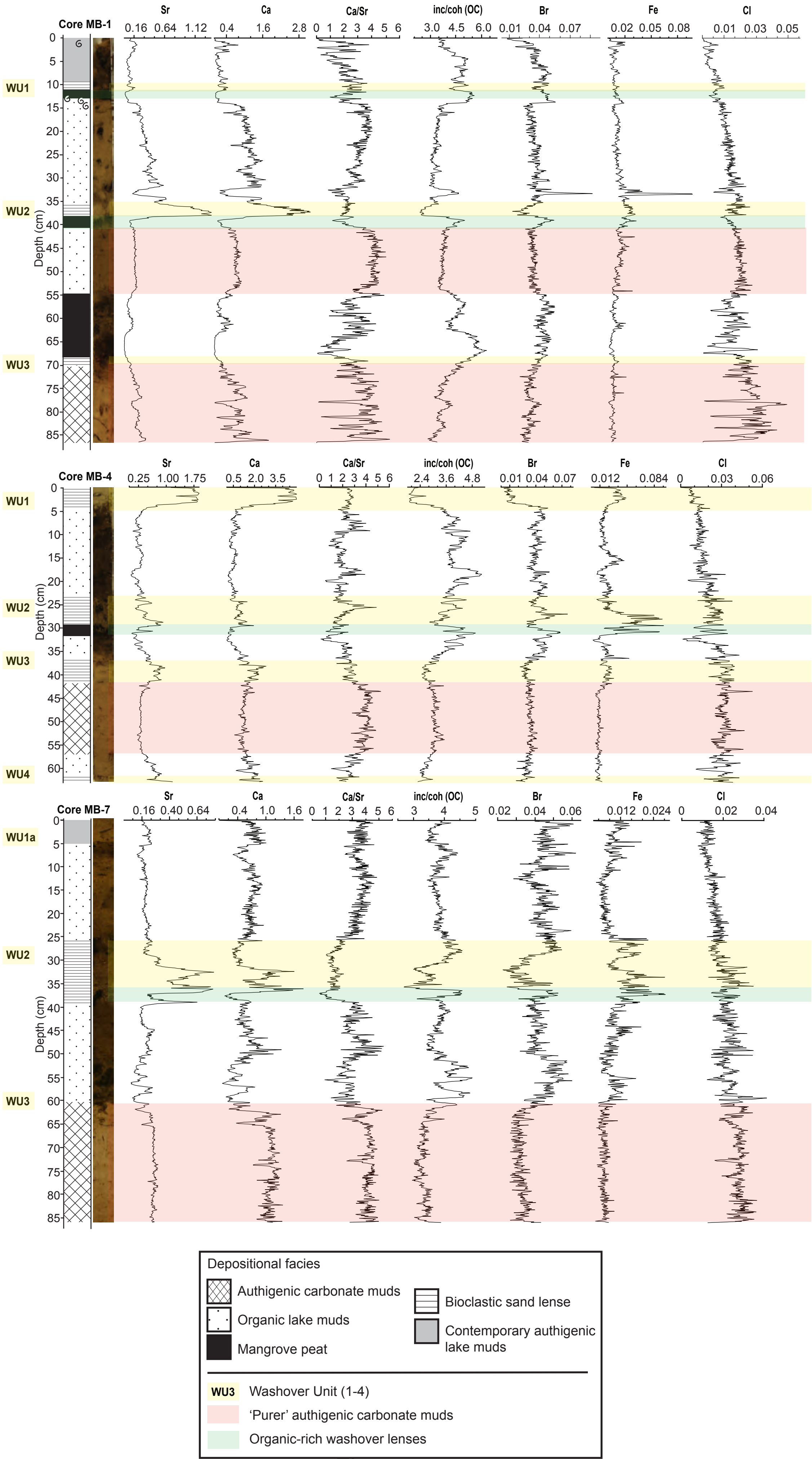
Core MB-1
Sr
Ca
Ca/Sr
inc/coh (OC)
Br
Fe
Cl
WU1
WU2
WU3
Depth (cm)
Core MB-4
WU4
Core MB-7
WU1a
Depositional facies
Authigenic carbonate muds
Organic lake muds
Mangrove peat
Bioclastic sand lense
Contemporary authigenic lake muds
Washover Unit (1-4)
'Purer' authigenic carbonate muds
Organic-rich washover lenses

Figure 5

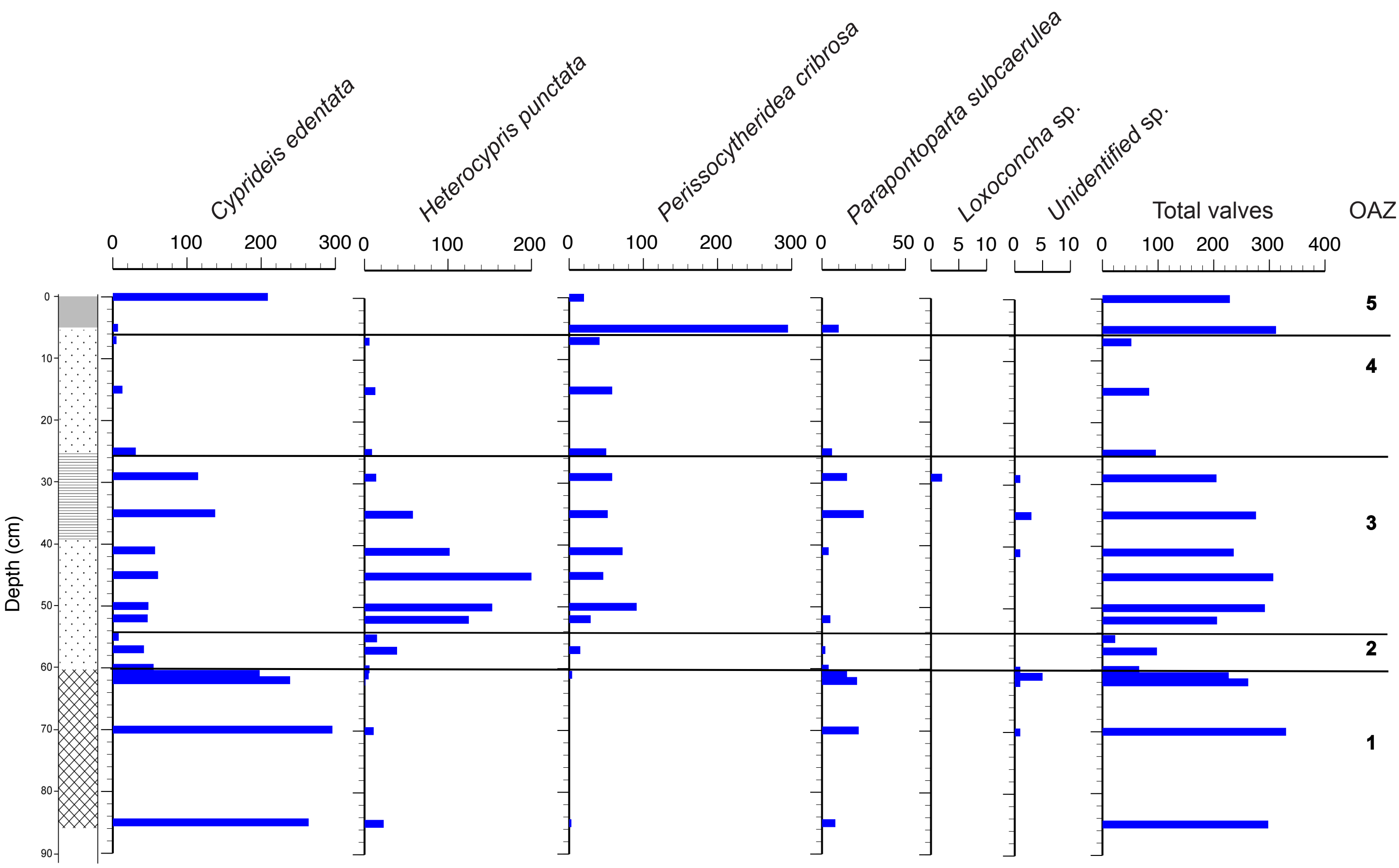

Cyprideis edentata
Heterocypris punctata
Perissocytheridea cribrosa
Parapontoparta subcaerulea
Loxoconcha sp.
Unidentified sp.
Total valves
OAZ
Depth (cm)
5
4
3
2
1

Figure 6

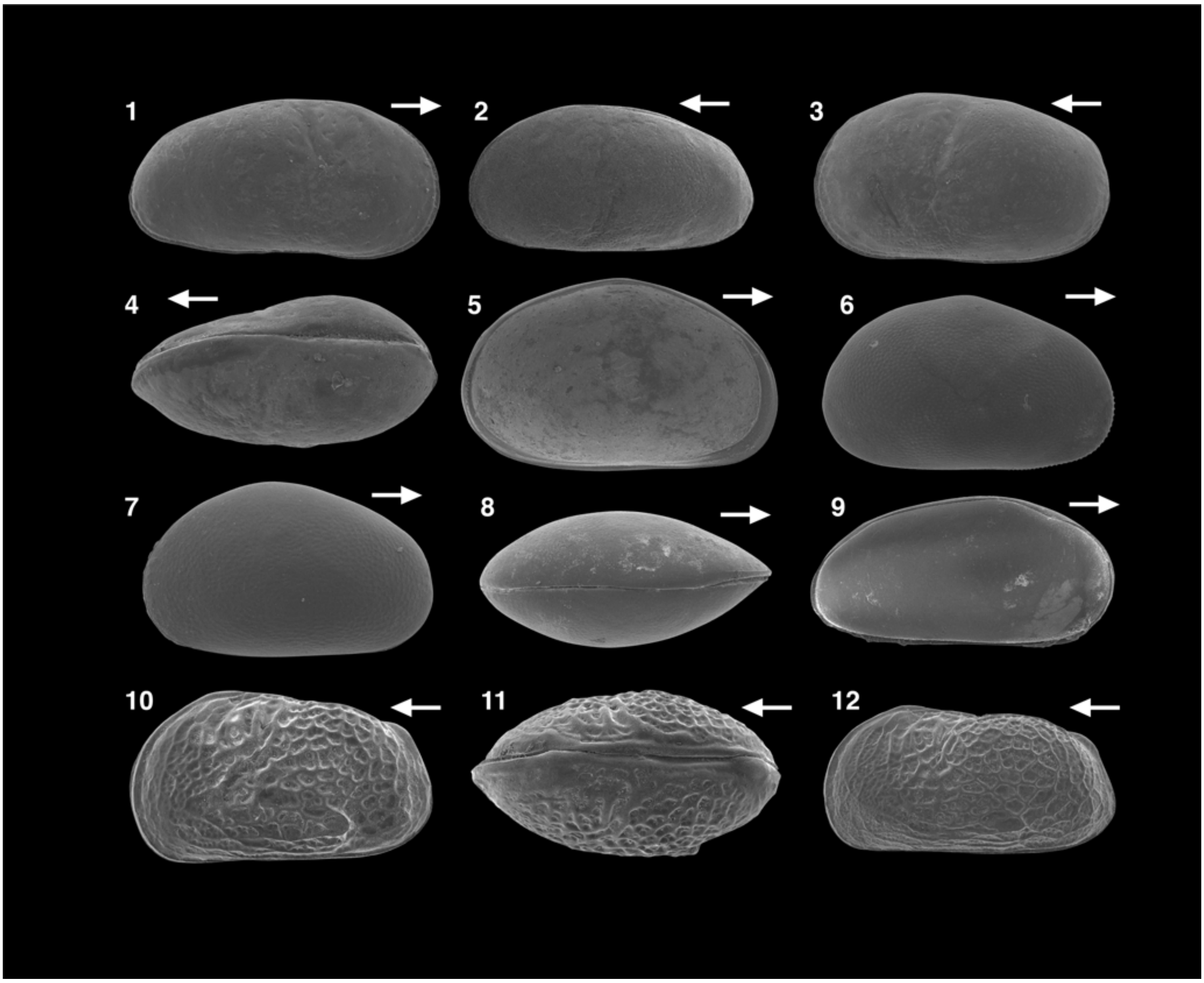

Figure 7

Table 1

Lab code	Core	Material	Depth (cm)	$\delta^{13}C$ (‰)	Age (14C yr BP)	2σ Calibrated cal AD	Probability (%)
Beta - 300722	MB-1	Articulated bivalve	90	-6.8	1100 +/- 30 BP	886-1013	95.4
Beta - 300723	MB-4	Bulk organics	34	-25.4	70 +/- 30 BP	1691-1730	24.3
						1810-1924	71.1
Beta - 336501	MB-7	*Ruppia* achenes	39-40	-22.0	620 +/- 30 BP	1292-1401	95.4
Beta - 336502	MB-7	*Ruppia* achenes	86-87	-18.7	1180 +/- 30 BP	730-736	0.7
						768-900	87.5
						920-951	7.2
Beta - 336503	MB-12	Mangrove leaf fragments	72	-27.4	620 +/- 30 BP	1292-1401	95.4